Published for SISSA by Springer

Received: *September 15, 2024*
Accepted: *October 2, 2024*
Published: *October 25, 2024*

Leptogenesis in SO(10) with minimal Yukawa sector

K.S. Babu,[a] **Pasquale Di Bari,**[b] **Chee Sheng Fong**[c] **and Shaikh Saad**[d]

[a]*Department of Physics, Oklahoma State University, Stillwater, OK 74078, U.S.A.*
[b]*School of Physics and Astronomy, University of Southampton, Southampton, SO17 1BJ, U.K.*
[c]*Centro de Ciências Naturais e Humanas, Universidade Federal do ABC, 09.210-170, Santo André, SP, Brazil*
[d]*Department of Physics, University of Basel, Klingelbergstrasse 82, CH-4056 Basel, Switzerland*

E-mail: babu@okstate.edu, P.Di-Bari@soton.ac.uk, sheng.fong@ufabc.edu.br, shaikh.saad@unibas.ch

Abstract: In prior studies, a very minimal Yukawa sector within the SO(10) Grand Unified Theory framework has been identified, comprising of Higgs fields belonging to a real 10_H, a real 120_H, and a $\overline{126}_H$ dimensional representations. In this work, within this minimal framework, we have obtained fits to fermion masses and mixings while successfully reproducing the cosmological baryon asymmetry via leptogenesis. The right-handed neutrino (N_i) mass spectrum obtained from the fit is strongly hierarchical, suggesting that $B - L$ asymmetry is dominantly produced from N_2 dynamics while N_1 is responsible for erasing the excess asymmetry. With this rather constrained Yukawa sector, fits are obtained both for normal and inverted ordered neutrino mass spectra, consistent with leptonic CP-violating phase $\delta_{\rm CP}$ indicated by global fits of neutrino oscillation data, while also satisfying the current limits from neutrinoless double beta decay experiments. In particular, the leptonic CP-violating phase has a preference to be in the range $\delta_{\rm CP} \simeq (230 - 300)^\circ$. We also show the consistency of the framework with gauge coupling unification and proton lifetime limits.

Keywords: Baryo-and Leptogenesis, Grand Unification

ArXiv ePrint: 2409.03840

https://doi.org/10.1007/JHEP10(2024)190

JHEP10(2024)190

Contents

1 Introduction

The Standard Model (SM) of particle physics is incredibly successful in describing the fundamental particles and their interactions. However, it does have some limitations and drawbacks. The model does not account for dark matter, it fails to incorporate the observed matter-antimatter asymmetry, and it predicts neutrinos to be massless, in contradiction with experiments. Several parameters of the model, such as fermion masses, mixing angles and the number of families, are adjusted to experimental observations and lack a fundamental explanation, leading to the well-known flavor puzzle.

Addressing these limitations is a significant focus of modern theoretical physics, with various models beyond the SM aiming at explaining some or all of these shortcomings. Grand Unified Theories (GUTs) [1–5] are well-motivated extensions which attempt such an explanation. GUTs unify three of the fundamental forces of nature, characterized by the SM gauge groups $\mathrm{SU}(3)_c \times \mathrm{SU}(2)_L \times \mathrm{U}(1)_Y$ into a single force arising from a simple group such as SU(5) and SO(10). GUTs also unify quarks and leptons [6] into common multiplets and explain the small neutrino masses via the seesaw mechanism [7–13]. Furthermore, GUTs shine in simplicity and elegance by reducing the number of effective parameters through which non-trivial correlations are obtained among the observed fermion masses and mixing angles. Finally, GUTs make testable predictions, such as proton decay, which provide concrete ways to confront these theories.

Among possible GUT gauge groups, SO(10) is arguably the most attractive candidate since it unifies all fermions of a generation into a single spinorial 16-dimensional representation.

Additionally, the spinorial representation contains the right-handed neutrino, which, via the seesaw mechanism, provides the desired tiny masses to the light neutrinos. Remarkably, in the decay of these same right-handed neutrinos to leptons and the SM Higgs, an asymmetry in the lepton number is generated, a process termed leptogenesis [14], which through electroweak sphaleron processes [15–17] gets partially converted into baryon asymmetry — hence explaining the observed matter-antimatter asymmetry of the Universe. (For reviews on leptogenesis, see for example refs. [18–26].) Moreover, it turns out that the Yukawa sector of SO(10) GUTs can be very predictive, which has been extensively analyzed in the literature [27–52] to study correlations among quark and lepton masses and mixings as well as neutrino oscillation parameters.

The focus of this paper is leptogenesis in a class of SO(10) GUTs with a very minimal Yukawa sector *without assuming additional symmetries.* Symmetries exterior to SO(10), such as flavor U(1), Peccei-Quinn U(1) and CP symmetry have been utilized in other studies in order to reduce the number of parameters. The Yukawa couplings of the models that we study here is based only on SO(10) symmetry and involve scalar fields belonging *real* 10_H, a real 120_H and a complex 126_H [43]. Such a system, which contains 15 moduli and 12 phases, has been shown to result in realistic fermion masses and mixings. Here we show that this setup can also generate the right amount of matter-antimatter asymmetry of the Universe via leptogenesis.

While light neutrino mass can arise from both type-I and type-II seesaw mechanisms, we focus here on the type-I dominated scenario (a pure type-II scenario, however, is incompatible with the observed fermion spectrum in this setup [43]). Due to the very constraining Yukawa sector, a good fit to fermion observables predicts a hierarchical mass spectrum of right-handed neutrinos N_i $(i = 1, 2, 3)$ with respective masses[1] $(M_1, M_2, M_3) \sim (10^{4-5}, 10^{11-12}, 10^{14-15})$ GeV. This is in accordance with the expectations of various SO(10)-inspired models [55–68]. This results in an interesting scenario where the final $B-L$ asymmetry is dominantly generated by the decays of the next-to-lightest right-handed neutrino, N_2, while the lightest right-handed neutrino, N_1, inverse decays wash-out the asymmetry at lower temperatures [69]. Thanks to flavor effects, the N_1-wash-out is strongly reduced [70] and in our case a sizeable part of the asymmetry produced from N_2-decays can survive the N_1 wash-out in the muon flavor. We show that this in accordance with the general analytical results from SO(10)-inspired leptogenesis scenarios [60].

Within the framework of SO(10) GUTs, baryogenesis via leptogenesis has been discussed in a series of works. In the SO(10)-inspired scenarios studied in refs. [55–68] leptogenesis is analyzed in a general framework without having a predictive fermion spectrum. The fermion mass spectrum and leptogenesis has been studied in tandem in refs. [49, 52, 71, 72]. In particular, refs. [49, 52, 71] have considered leptogenesis in $\mathrm{SO}(10) \times \mathrm{U}(1)_{PQ}$ models with the Yukawa sector consisting of scalar fields belonging to a complex 10_H and a 126_H. This model gives rise to a more compact spectrum of right-handed neutrinos where their masses fall within the range $M_i \sim (10^9 - 10^{12})$ GeV and leptogenesis can have relevant contributions from decays of some or all N_i. On the other hand, ref. [72] has considered leptogenesis

[1]As is well known [53, 54], heavy right-handed neutrinos with masses on the order of 10^7 GeV contribute to the Higgs mass through loop corrections, which contributes to the hierarchy problem. However, in grand unified theories, fine-tuning of quadratically divergent contributions is typically required to adjust the Higgs mass.

JHEP10(2024)190

with the same scalar field content but with $SO(10) \times CP$ where the discrete CP symmetry makes all Yukawa couplings to be real, thus reducing the number of parameters. In such a model, the spectrum of right-handed neutrinos is strongly hierarchical with $M_1 \sim 10^7$ GeV $\ll M_2 \ll M_3 \sim 10^{12}$ GeV such that leptogenesis proceeds mainly through decays of N_2 while N_1 erases part of the asymmetry generated. In contrast to these works, the present work assumes no additional symmetries beyond SO(10) gauge symmetry.

By performing a detailed numerical analysis, we show that leptogenesis is viable for both normal and inverted mass ordering of light neutrinos. In particular, the value of the leptonic Dirac CP phase $\delta_{\rm CP}$ is consistent, both for normal and inverted mass ordering, with the current global fits, which mildly prefer nonzero $\delta_{\rm CP}$ [73]. Since we aim for precision calculation, we utilize lepton-flavor-covariant formalism (i.e. independent of lepton flavor basis) developed in ref. [74] which takes into account both lepton flavor effects [25] and spectator effects [75, 76]. The renormalization-group running effect is partially taken into account by considering two sets of Yukawa couplings, one at the scale M_2, the mass scale of N_2, and the other at the scale M_1 with the appropriate matching conditions imposed. While the model admits both normal ordering (NO) and inverted ordering (IO) of neutrino masses, recent global fits and cosmological constraints show a preference to NO, which we analyze in more detail. In this case, the leptonic CP-violating phase is found, in our fit, to have a preferred value in the range $\delta_{\rm CP} \simeq (230 - 300)^\circ$. The best fit values of the parameters that explain simultaneously the fermion mass spectrum and the baryon asymmetry are listed in table 1.

Our analysis reveals that for gauge coupling unification, it is crucial to incorporate some amount of threshold corrections to achieve large enough unification scale to be compatible with proton lifetime limits. Without these threshold corrections which arise from scalar sub-multiplets, proton lifetime would be too rapid and inconsistent with the current experimental bounds. A dedicated analysis is carried out to show the consistency of the model with gauge coupling unification and proton lifetime limits. Interestingly, the model prefers the lifetime to be on the lower end, which experiments such as Hyper-Kamiokande are expected to probe.

The rest of the article is organized as follows. In section 2, we introduce the model, and in section 3, we provide all the necessary details to perform leptogenesis computation. In section 4, we undertake an extensive numerical analysis in search of finding a consistent fits of the fermion masses and mixings as well as reproducing the correct baryon asymmetry parameters. In section 5 we provide some insights into the calculation of the asymmetry, comparing our numerical results to the analytical results from SO(10)-inspired leptogenesis [64, 66, 68]. A detailed analyses of gauge coupling unification and proton decay is carried out in section 6. Finally, we conclude in section 7.

2 Minimal Yukawa sector

Assuming that there are no additional fermions beyond the three families of chiral spinorial representation of SO(10), the following fermion bilinear specifies the possible Higgs representations that can contribute to the fermion mass generation in a renormalizable theory:

$$16 \times 16 = 10_s + 120_a + 126_s. \tag{2.1}$$

Here the subscripts s and a represent symmetric and antisymmetric components in family space. Note that 10- and 120-dimensional representations are real, whereas 126-dimensional representation is inherently complex. With the above bilinears, the most general Yukawa sector of renormalizable SO(10) GUTs can be written as

$$\mathcal{L}_{yuk} = 16_F (y_{10}^p 10_H^p + y_{120}^q 120_H^q + y_{126}^r \overline{126}_H^r) 16_F. \tag{2.2}$$

In the above equation, we have suppressed the family index. If n_{10} copies of 10-dimensional representations are present, then the index p takes values $p = 1, 2, \dots, n_{10}$; similarly $q = 1, 2, \dots, n_{120}$ and $r = 1, 2, \dots, n_{126}$. Each Yukawa coupling Y_{10} (and Y_{126}) is a symmetric 3×3 matrix in the family space, whereas Y_{120} is antisymmetric.

It turns out that viable fermion spectrum can only be generated provided for $n_{10} + n_{120} + n_{126} > 2$. By considering various possibilities, ref. [43] identified that the most minimal Yukawa sector corresponds to $(n_{10}, n_{120}, n_{126}) = (1, 1, 1)$. In this scenario, one has two symmetric and one antisymmetric Yukawa matrices, leading to a total of 3 real plus 9 complex Yukawa parameters. Note that either y_{10} or y_{126} can be made real and diagonal using an SO(10) rotation, which has been used for the parameter counting. If any other realistic choice is considered, for example, $(n_{10}, n_{120}, n_{126}) = (2, 0, 1)$, then one would end up with larger number of parameters, viz., 3 real and 12 complex Yukawa parameters for this choice.

There is an alternative option to reduce the number of Yukawa parameters, which however, requires extending the symmetry of the theory. Along this line, the most studied case in the literature is $(n_{10}, n_{120}, n_{126}) = (2, 0, 1)$, where two 10-dimensional representations are complexified using a Peccei-Quinn $\mathrm{U}(1)_{\mathrm{PQ}}$. In this construction, only one of the two Yukawa couplings associated to 10_H is allowed due to the PQ symmetry, thereby reducing 6 complex Yukawa parameters [27].

In this work, we stick to the scenario where the full symmetry of the theory is nothing but SO(10) gauge symmetry, and consider the most minimal Yukawa sector that corresponds to $(n_{10}, n_{120}, n_{126}) = (1, 1, 1)$. Then, the up-type quark, down-type quark, charged leptons, Dirac neutrino, and Majorana neutrino mass matrices can be written as [43]:

$$M_U = \underbrace{v_{10} y_{10}}_{\equiv D} + \underbrace{v_{126}^u y_{126}}_{\equiv S} + \underbrace{(v_{120}^{(1)} + v_{120}^{(15)}) y_{120}}_{\equiv A}, \tag{2.3}$$

$$M_D = v_{10}^* y_{10} + v_{126}^d y_{126} + (v_{120}^{(1)*} + v_{120}^{(15)*}) y_{120}, \tag{2.4}$$

$$M_E = v_{10}^* y_{10} - 3 v_{126}^d y_{126} + (v_{120}^{(1)*} - 3 v_{120}^{(15)*}) y_{120}, \tag{2.5}$$

$$M_{\nu_D} = v_{10} y_{10} - 3 v_{126}^u y_{126} + (v_{120}^{(1)} - 3 v_{120}^{(15)}) y_{120}, \tag{2.6}$$

$$M_{\nu_R} = v_R y_{126}. \tag{2.7}$$

There are a few special features of the above set of mass matrices. For example, the same VEV (vacuum expectation value) v_{10} enters in both the up-sector (up-type quark and Dirac neutrino) as well as in the down-sector (down-type quark and charged lepton). This happens because 10_H is a real representation and it contains a self-conjugate bi-doublet, $(1, 2, 2)$, under the $\mathrm{SU}(4)_c \times \mathrm{SU}(2)_L \times \mathrm{SU}(2)_R$ (Pati-Salam) subgroup of SO(10). Consequently, the reality of 10_H implies that $v_u = v_d^* \equiv v_{10}$. Additionally, the reality of 120_H implies, $v_u^{(1)} = v_d^{(1)*} \equiv v_{120}^{(1)}$ and $v_u^{(15)} = v_d^{(15)*} \equiv v_{120}^{(15)}$. Here $v_{120}^{(1)}$ and $v_{120}^{(15)}$ represent the VEVs of the submultiplets $(1, 2, 2)$ and $(15, 2, 2)$ contained in 120_H, under the Pati-Salam symmetry. The VEVs of the up-type and down-type weak doublets contained in $(15, 2, 2)$ arising from the complex 126_H, which we denote by v^u_{126} and v^d_{126}, have no such relations. We now define

$$r_1 = \frac{v^d_{126}}{v^u_{126}}, \quad r_2 = \frac{v^{(1)*}_{120} - 3v^{(15)*}_{120}}{v^{(1)}_{120} + v^{(15)}_{120}}, \quad e^{i\phi} = \frac{v^{(1)*}_{120} + v^{(15)*}_{120}}{v^{(1)}_{120} + v^{(15)}_{120}}, \quad c_R = \frac{v_R}{v^u_{126}}, \tag{2.8}$$

and rewrite the above mass matrices as

$$M_U = \underbrace{D}_{\text{symetric}} + \underbrace{S}_{\text{real}-\text{diagonal}} + \underbrace{A}_{\text{antisymetric}} \equiv v y_U, \tag{2.9}$$

$$M_D = D + r_1 S + e^{i\phi} A \equiv v y_D, \tag{2.10}$$

$$M_E = D - 3r_1 S + r_2 A \equiv v y_E, \tag{2.11}$$

$$M_{\nu_D} = D - 3S + r_2^* e^{i\phi} A \equiv v y_{\nu_D}, \tag{2.12}$$

$$M_{\nu_R} = c_R S, \tag{2.13}$$

with $v^2 = |v_{10}|^2 + |v^{(1)}_{120}|^2 + |v^{(15)}_{120}|^2 + |v^u_{126}|^2 + |v^d_{126}|^2$, and $v = 174.104\,\text{GeV}$. These Yukawa coupling matrices, y_f, (with $f = U, D, E, \nu_D$) are matched to the following Lagrangian of the SM extended with right-handed neutrinos:

$$-\mathcal{L}_{yuk} = (y_{\nu_D})_{ij}\overline{N_i}\ell_j\epsilon H + (y_U)_{ij}\overline{U_i}Q_j\epsilon H + (y_D)_{ij}\overline{D_i}Q_j H^* + (y_E)_{ij}\overline{E_i}\ell_j H^* + \frac{1}{2}(M_{\nu_R})_{ii}\overline{N_i}N_i^c + \text{h.c.}, \tag{2.14}$$

where Q_j, ℓ_j and H are the left-handed quark, lepton and Higgs $\mathrm{SU}(2)_L$ doublets, respectively; U_i, D_i, E_i and N_i are the right-handed up-type quark, down-type quark, charged lepton and neutrino $\mathrm{SU}(2)_L$ singlets, respectively, $i, j = 1, 2, 3$ are the family indices, the superscript c denotes charge conjugation and ϵ is the antisymmetric tensor for $\mathrm{SU}(2)_L$ contraction.

Here we have chosen a phase convention where v_{10} is made real by an $\mathrm{SU}(2)_L$ rotation. Without loss of generality, we choose to work in a basis where the matrix S is diagonal and real, as specified above. When the charged fermion Yukawa coupling matrices are diagonalized, the corresponding diagonal couplings are denoted by $y_U^{\text{diag}} = (y_u, y_c, y_t)$, $y_D^{\text{diag}} = (y_d, y_s, y_b)$, and $y_E^{\text{diag}} = (y_e, y_\mu, y_\tau)$. The light neutrino mass matrix m_ν for the SM neutrinos ν_i, obtained from the seesaw formula [7–11], in the basis $\overline{\nu^c}\, m_\nu\, \nu/2$ is given by,

$$m_\nu = -M^T_{\nu_D} M^{-1}_{\nu_R} M_{\nu_D}, \tag{2.15}$$

where we have assumed the type-I dominance. We diagonalize the neutrino mass matrix as follows:

$$m_\nu = N_L^* \text{diag}(m_1, m_2, m_3) N_L^\dagger, \tag{2.16}$$

where N_L is a unitary matrix. Then, the PMNS matrix is defined as

$$U_\nu = E_L^\dagger N_L, \tag{2.17}$$

where the unitary matrix E_L is obtained by diagonalizing the charged lepton mass matrix $M_E = E_R\,\mathrm{diag}(m_e, m_\mu, m_\tau)E_L^\dagger$ where E_R is the right-handed analog of E_L. We parametrize the Pontecorvo-Maki-Nakagawa-Sakata (PMNS) matrix as:

$$U_\nu = \begin{pmatrix} c_{12}\,c_{13} & s_{12}\,c_{13} & s_{13}\,e^{-\mathrm{i}\,\delta_{\mathrm{CP}}} \\ -s_{12}\,c_{23} - c_{12}\,s_{23}\,s_{13}\,e^{\mathrm{i}\,\delta_{\mathrm{CP}}} & c_{12}\,c_{23} - s_{12}\,s_{23}\,s_{13}\,e^{\mathrm{i}\,\delta_{\mathrm{CP}}} & s_{23}\,c_{13} \\ s_{12}\,s_{23} - c_{12}\,c_{23}\,s_{13}\,e^{\mathrm{i}\,\delta_{\mathrm{CP}}} & -c_{12}\,s_{23} - s_{12}\,c_{23}\,s_{13}\,e^{\mathrm{i}\,\delta_{\mathrm{CP}}} & c_{23}\,c_{13} \end{pmatrix} \times \mathrm{diag}(e^{-i\alpha/2}, e^{-i\beta/2}, 1), \tag{2.18}$$

where $c_{ij} = \cos\theta_{ij}$ and $s_{ij} = \sin\theta_{ij}$.

The number of parameters contained in the fermion mass matrices given in eqs. (2.9)–(2.13) may be counted as follows. Matrices S, A, and D contain 3 real, 3 complex, and 6 complex parameters, respectively. The ratios $r_{1,2}$ are complex, whereas, the phase of c_R is irrelevant for fermion mass fit. Moreover, there is a non-trivial phase, ϕ, as defined in eq. (2.8). Altogether, we have 15 real parameters and 12 phases. If all parameters were real, then these 15 real parameters would determine 17 observables, namely, 9 charged fermion masses, 3 quark mixing angles, 2 neutrino mass-squared differences, and 3 neutrino mixing angles. Such a system, however, would not explain the observed CP violation in the quark sector, and also would not lead to a realistic fermion spectrum. Hence the phases play a crucial role in providing a correct fit to the masses and mixings. Since 12 of the parameters are phases, it is nontrivial to achieve a consistent fit.

3 Leptogenesis

Aiming to determine the production of baryon asymmetry from leptogenesis as precise as possible, we will utilize the lepton-flavor-covariant formalism developed in ref. [74] which includes both lepton flavor effects [25] and spectator effects [75, 76]. The renormalization-group-running effects will also be partially taken into account as described at the end of this section. First we review the formalism used in this work.

Let us define the number asymmetry of particle species i as

$$Y_{\Delta i} \equiv Y_i - Y_{\bar{i}} = \frac{n_i}{s} - \frac{n_{\bar{i}}}{s}, \tag{3.1}$$

where $n_{i(\bar{i})}$ is particle (antiparticle) number density of species i and $s = \frac{2\pi^2}{45} g_\star T^3$ is the cosmic entropy density and $g_\star$ is the effective relativistic degrees of freedom of the Universe at the relevant temperature. The baryon number charge (B) can be constructed as

$$Y_B = \sum_i q_i^B Y_{\Delta i}, \tag{3.2}$$

where q_i^B is the baryon number carried by species i.

Since we are interested in taking into account lepton flavor effects, we will consider 3×3 matrices of number asymmetries of lepton doublets ℓ and charged lepton singlet E, $Y_{\Delta\ell}$ and $Y_{\Delta E}$

$$Y_{\Delta\ell} = \begin{pmatrix} Y_{\Delta\ell_{11}} & Y_{\Delta\ell_{12}} & Y_{\Delta\ell_{13}} \\ Y^*_{\Delta\ell_{12}} & Y_{\Delta\ell_{22}} & Y_{\Delta\ell_{23}} \\ Y^*_{\Delta\ell_{13}} & Y^*_{\Delta\ell_{23}} & Y_{\Delta\ell_{33}} \end{pmatrix}, \quad Y_{\Delta E} = \begin{pmatrix} Y_{\Delta E_{11}} & Y_{\Delta E_{12}} & Y_{\Delta E_{13}} \\ Y^*_{\Delta E_{12}} & Y_{\Delta E_{22}} & Y_{\Delta E_{23}} \\ Y^*_{\Delta E_{13}} & Y^*_{\Delta E_{23}} & Y_{\Delta E_{33}} \end{pmatrix}, \tag{3.3}$$

where the basis-independent quantities $\mathrm{Tr}\,(Y_{\Delta\ell})$ and $\mathrm{Tr}\,(Y_{\Delta E})$ are respectively the total number asymmetries of lepton doublets ℓ and charged lepton singlet E. The off-diagonal elements are needed to describe lepton flavor coherence and correlations.

Let us further define the following baryon charge matrix

$$Y_{\widetilde{\Delta}} \equiv \frac{1}{3} Y_B I_{3\times 3} - Y_{\Delta\ell}. \tag{3.4}$$

The evolution of $Y_{\widetilde{\Delta}}$ due to the SM charged lepton Yukawa interactions can be described by

$$s\mathcal{H}z \frac{dY_{\widetilde{\Delta}}}{dz} = \frac{\gamma_E}{2Y^{\mathrm{nor}}} \left\{ y_E^\dagger y_E, \frac{Y_{\Delta\ell}}{g_\ell \zeta_\ell} \right\} - \frac{\gamma_E}{Y^{\mathrm{nor}}} y_E^\dagger y_E \frac{Y_{\Delta H}}{g_H \zeta_H} - \frac{\gamma_E}{Y^{\mathrm{nor}}} y_E^\dagger \frac{Y_{\Delta E}}{g_E \zeta_E} y_E \tag{3.5}$$

where we have defined the anticommutator $\{\mathcal{A}, \mathcal{B}\} \equiv \mathcal{AB} + \mathcal{BA}$, $z \equiv M_{\mathrm{ref}}/T$ with M_{ref} an arbitrary mass scale, $\mathcal{H} = 1.66\sqrt{g_\star} T^2/M_{\mathrm{Pl}}$ with $M_{\mathrm{Pl}} = 1.22 \times 10^{19}$ GeV is the Hubble rate during the radiation dominated era, $Y^{\mathrm{nor}} \equiv \frac{15}{8\pi^2 g_\star}$, g_i is the gauge degrees of freedom of species i (with $g_\ell = g_H = 2$ and $g_E = 1$) and

$$\zeta_i \equiv \frac{6}{\pi^2} \int_{m_i/T}^{\infty} dx\, x\sqrt{x^2 - m_i^2/T^2} \frac{e^x}{(e^x + \xi_i)^2}, \tag{3.6}$$

with m_i the mass of i and $\xi_i = 1(-1)$ for fermion (boson). Since we are considering the condition before electroweak symmetry breaking, we will take $m_\ell = m_E = m_H = 0$ which results in $\zeta_\ell = \zeta_E = \zeta_H/2 = 1$. The charged lepton Yukawa reaction density γ_E was determined in refs. [77, 78] to be $\gamma_E \approx 5 \times 10^{-3} \frac{T^4}{6}$, which we shall make use of.

Assuming that the electroweak sphaleron freezes out at 132 GeV after the electroweak phase transition temperature of 160 GeV [79], we obtain the final baryon charge asymmetry as

$$Y_B = c_{sp}(T) \mathrm{Tr}(Y_{\widetilde{\Delta}} - Y_{\Delta E})\big|_{T=132\,\mathrm{GeV}} \tag{3.7}$$

where assuming the SM degrees of freedom, we have [80]

$$c_{sp}(T) = \frac{6(5+\zeta_t)}{97+14\zeta_t}. \tag{3.8}$$

The extreme values of this parameter are $c_{sp} = 12/37$ for $\zeta_t = 1$ and $c_{sp} = 30/97$ for $\zeta_t = 0$. Using the top mass $m_t = 173$ GeV, we have $c_{sp} = 0.315$ which is the value we will use. To convert to $\eta_B \equiv n_B/n_\gamma$ i.e. the baryon number density normalized to the photon number density today, we multiply Y_B by the ratio of entropy to photon number density today $s_0/n_{\gamma 0} = 7.039$.

From eq. (2.14), we can write down the relevant type-I seesaw Lagrangian with $M_i \equiv (M_{\nu_R})_{ii}$ and $y \equiv y_{\nu D}$ in the mass basis of N_i as follows:

$$-\mathcal{L} \supset \frac{1}{2} M_i \overline{N_i} N_i^c + y_{i\alpha} \overline{N_i} \ell_\alpha \epsilon H + (y_E)_{\alpha\beta} \overline{E_\alpha} \ell_\beta H^* + \mathrm{h.c.}, \tag{3.9}$$

where lepton number L or $B-L$ are explicitly broken, and for readability we have used Greek indices $\alpha, \beta = 1,2,3$ to denote the SM lepton flavors to distinguish them from the flavors of N_i $(i = 1,2,3)$. The evolution of Y_{N_i} is described by

$$s\mathcal{H}z \frac{dY_{N_i}}{dz} = -\gamma_{N_i} \left(\frac{Y_{N_i}}{Y_{N_i}^{\mathrm{eq}}} - 1 \right), \tag{3.10}$$

JHEP10(2024)190

where we now fix the reference scale by defining $z \equiv M_1/T$. In our calculations, we assume that the SO(10) GUT is broken before/during the inflation and after inflation, the reheat temperature T_R is below the GUT scale, so that the GUT gauge bosons are not brought into thermal equilibrium. We can estimate if N_i will be thermalized through GUT gauge interaction by estimating the relevant rate by

$$\Gamma_R \sim \frac{T^5}{\pi^3 v_R^4}. \tag{3.11}$$

Comparing to the Hubble rate $\mathcal{H}(T)$ assuming radiation domination, N_i will be thermalized if the cosmic temperature satisfies

$$T > T_{eq} \sim 1.6 \times 10^{13}\,\text{GeV} \left(\frac{v_R}{10^{14}\,\text{GeV}}\right)^4, \tag{3.12}$$

where we have set $g_\star = 106.75$. If $T_R < T_{eq}$ or $M_i > T_{eq}$, N_i will not be thermalized. Since T_R and also v_R are unknown, we will quote the results for the baryon asymmetry assuming zero and thermal initial abundances of N_i in the next section.

Next, to eq. (3.5), we introduce a source and a washout term respectively given by[2]

$$S^{\text{I}} \equiv -\sum_i \epsilon_i \gamma_{N_i} \left(\frac{Y_{N_i}}{Y_{N_i}^{\text{eq}}} - 1\right), \tag{3.13}$$

$$W^{\text{I}} \equiv \frac{1}{2}\sum_i \frac{\gamma_{N_i}}{Y^{\text{nor}}} \left(\frac{1}{2}\left\{P_i, \frac{Y_{\Delta\ell}}{g_\ell \zeta_\ell}\right\} + P_i \frac{Y_{\Delta H}}{g_H \zeta_H}\right). \tag{3.14}$$

We will further assume Maxwell-Boltzmann distribution to calculate the decay reaction density,

$$\gamma_{N_i} = s Y_{N_i}^{\text{eq}} \Gamma_{N_i} \frac{\mathcal{K}_1 (M_i/T)}{\mathcal{K}_2 (M_i/T)}, \tag{3.15}$$

where $Y_{N_i}^{\text{eq}} = \frac{45}{2\pi^4 g_\star} \frac{M_i^2}{T^2} \mathcal{K}_2 \left(\frac{M_i}{T}\right)$ with $\mathcal{K}_n(x)$ the modified Bessel function of the second kind of order n and $\Gamma_{N_i} = \frac{(yy^\dagger)_{ii} M_i}{8\pi}$ is the total decay width of N_i. The CP parameter matrix ϵ_i and flavor projection matrix P_i are respectively given by [81]

$$\begin{aligned}(\epsilon_i)_{\alpha\beta} = &\frac{1}{16\pi} \frac{i}{(yy^\dagger)_{ii}} \sum_{j\neq i} \left[\left(yy^\dagger\right)_{ji} y_{j\beta} y_{i\alpha}^* - \left(yy^\dagger\right)_{ij} y_{i\beta} y_{j\alpha}^*\right] g\left(\frac{M_j^2}{M_i^2}\right) \\ &+ \frac{1}{16\pi} \frac{i}{(yy^\dagger)_{ii}} \sum_{j\neq i} \left[\left(yy^\dagger\right)_{ij} y_{j\beta} y_{i\alpha}^* - \left(yy^\dagger\right)_{ji} y_{i\beta} y_{j\alpha}^*\right] \frac{M_i^2}{M_i^2 - M_j^2},\end{aligned} \tag{3.16}$$

$$P_i = \frac{1}{(yy^\dagger)_{ii}} \begin{pmatrix} |y_{i1}|^2 & y_{i1}^* y_{i2} & y_{i1}^* y_{i3} \\ y_{i1} y_{i2}^* & |y_{i2}|^2 & y_{i2}^* y_{i3} \\ y_{i1} y_{i3}^* & y_{i2} y_{i3}^* & |y_{i3}|^2 \end{pmatrix}, \tag{3.17}$$

where

$$g(x) \equiv \sqrt{x}\left[\frac{1}{1-x} + 1 - (1+x)\ln\frac{1+x}{x}\right]. \tag{3.18}$$

[2] We will consider only decay and inverse decay of N_i since scatterings are in general suppressed.

Under arbitrary flavor rotations

$$E \to U_E E, \quad \ell \to V_\ell \ell, \quad y \to y V_\ell^\dagger, \quad y_E \to U_E y_E V_\ell^\dagger, \tag{3.19}$$

where U_E and V_ℓ are unitary matrices, the density matrix of eq. (3.5), including the source and washout terms of eqs. (3.13)–(3.14), is manifestly covariant with

$$Y_{\Delta\ell} \to V_\ell Y_{\Delta\ell} V_\ell^\dagger, \quad Y_{\Delta E} \to U_E Y_{\Delta E} U_E^\dagger, \tag{3.20}$$

$$\epsilon_i \to V_\ell \epsilon_i V_\ell^\dagger, \qquad P_i \to V_\ell P_i V_\ell^\dagger. \tag{3.21}$$

From eq. (3.7), we see that the B or $B-L$ asymmetry at any moment is invariant under such rotations.

To have closed set of equations, we can write [74]

$$Y_{\Delta\ell} = \frac{2}{15} c_B \mathrm{Tr} Y_{\widetilde{\Delta}} - Y_{\widetilde{\Delta}}, \tag{3.22}$$

$$Y_{\Delta H} = -c_H \left(\mathrm{Tr} Y_{\widetilde{\Delta}} - 2\mathrm{Tr} Y_{\Delta E} \right), \tag{3.23}$$

where $Y_{\Delta\ell}$ is now a 3×3 matrix with off-diagonal element $\alpha \neq \beta$ given by $(Y_{\Delta\ell})_{\alpha\beta} = -\left(Y_{\widetilde{\Delta}}\right)_{\alpha\beta}$. The temperature-dependent coefficients c_B and c_H can capture *all* the spectator effects in the SM. Across $T_B \sim 2\times10^{12}$ GeV, the EW sphaleron interaction gets into equilibrium. To within percent level precision, the following fitting function can be used [82]

$$c_B(T) = 1 - e^{-\frac{T_B}{T}}, \tag{3.24}$$

where $T_B = 2.3\times10^{12}$ GeV. The rest of the quark spectator effects are described by c_H with [82]

$$c_H(T) = \begin{cases} 1 & T > T_t \\ \frac{2}{3} & T_u < T < T_t \\ \frac{14}{23} & T_{u-b} < T < T_u \\ \frac{2}{5} & T_{u-c} < T < T_{u-b} \\ \frac{4}{13} & T_{B_3-B_2} < T < T_{u-c} \\ \frac{3}{10} & T_{u-s} < T < T_{B_3-B_2} \\ \frac{1}{4} & T_{u-d} < T < T_{u-s} \\ \frac{2}{11} & T < T_{u-d} \end{cases}, \tag{3.25}$$

where we use the transition temperatures T_x given in ref. [74]. One can parametrize these transitions with the following function:

$$\begin{aligned} c_H(T) = &\left(\frac{2}{3} + \frac{1}{3} e^{-\frac{T_t}{T}}\right) - \left(\frac{2}{3} - \frac{14}{23}\right)\left(1 - e^{-\frac{T_u}{T}}\right) - \left(\frac{14}{23} - \frac{2}{5}\right)\left(1 - e^{-\frac{T_{u-b}}{T}}\right) \\ &- \left(\frac{2}{5} - \frac{4}{13}\right)\left(1 - e^{-\frac{T_{u-c}}{T}}\right) - \left(\frac{4}{13} - \frac{3}{10}\right)\left(1 - e^{-\frac{T_{B_3-B_2}}{T}}\right) \\ &- \left(\frac{3}{10} - \frac{1}{4}\right)\left(1 - e^{-\frac{T_{u-s}}{T}}\right) - \left(\frac{1}{4} - \frac{2}{11}\right)\left(1 - e^{-\frac{T_{u-d}}{T}}\right). \end{aligned} \tag{3.26}$$

In the model under discussion, as we will see in the next section, due to the mass spectrum of N_i imposed by the model, N_2 is mainly responsible for asymmetry generation while N_1 dynamics is mainly responsible for washout and the role of N_3 is important in yielding the necessary interference to have non-vanishing CP violation in N_2 decays: it should be then appreciated how the existence of three families is crucial to have successful leptogenesis.

For the calculation of the final asymmetry, we partially take into account renormalization-group running by considering two sets of Yukawa couplings, one fixed at renormalization scale $\mu = M_2$ throughout N_2 leptogenesis while another is fixed at scale $\mu = M_1$ throughout N_1 washout. This running effect is important since the washout depends exponentially on the decay parameter defined as

$$K_i(\mu) \equiv \frac{\Gamma_{N_i}(\mu)}{\mathcal{H}(T = M_i)} \equiv \frac{(yy^\dagger)_{ii} v^2}{m_\star M_i}, \tag{3.27}$$

where $m_\star \equiv 1.66\sqrt{g_\star} \times 8\pi v^2/M_{\rm Pl}$ and $K_i > (<) 1$ is known as strong (weak) washout regime in which N_i does (not) thermalize before decay. The two sets of Yukawa couplings y and y_E in the right-handed neutrino mass basis at renormalization scale $\mu = M_2$ and $\mu = M_1$ are given in appendix C. One should have in mind that, despite a full account of flavor and spectator effects, in the intermediate to strong washout regimes (as indicated by our benchmark points in the next section), there remains a theoretical uncertainty of $\mathcal{O}(1)$ since we are not taking into account full running of parameters, as well as thermal and next-to-leading order corrections [83–85].

4 Numerical analysis

In this section, we perform a combined fit to the fermion masses and mixings along with the baryon asymmetry of the universe. In our fitting procedure, we first use the approximate formulas for the calculation of baryon asymmetry through leptogenesis as in ref. [81] to identify candidate points which might produce sufficient baryon asymmetry. Only after a good fit is obtained, we carry out a full numerical calculation for baryon asymmetry using the formalism explained in the previous section to see if the resulting baryon asymmetry is consistent with the observed value. The details of our fitting procedure are summarized below.

4.1 Benchmark fits

The free parameters $S_{ii}, D_{ij}^{j\geq i}, A_{ij}^{j>i}, r_{1,2,}, c_R$, and ϕ are varied randomly at the GUT scale, which we choose to be $M_{\rm GUT} = 2 \times 10^{16}$ GeV. We then run the relevant Yukawa couplings defined in eqs. (2.9)–(2.12) and the right-handed neutrino mass matrix of eq. (2.13) by taking into account the full SM+Type-I seesaw renormalization group equations (RGEs) from $M_{\rm GUT}$ to M_Z scale. In this running procedure, heavy right-handed neutrinos are successively integrated out at their respective mass thresholds. We have implemented our model in the package `REAP` [86] to take into account this running. Since the model under investigation predicts the intermediate symmetry breaking scale, $M_{\rm int} \sim 10^{14}$ GeV (as shown below), which is very close to the GUT scale, for our purpose, it is good enough to consider only SM+Type-I RGEs below the GUT scale. Note that to be consistent with the present experimental bounds [87] on gauge-mediated proton decay, the GUT scale approximately needs to satisfy $M_{\rm GUT} \gtrsim 5 \times 10^{15}$ GeV. Consistency of obtaining such a large intermediate scale as well as evading proton decay bounds are discussed in section 6.

JHEP10(2024)190

Observables (Δm_{ij}^2 in eV^2)	Values at M_Z scale		
	Input	Benchmark Fit: NO	Benchmark Fit: IO
$y_u/10^{-6}$	6.65±2.25	7.30	10.0
$y_c/10^{-3}$	3.60±0.11	3.59	3.57
y_t	0.986±0.0086	0.986	0.986
$y_d/10^{-5}$	1.645±0.165	1.636	1.635
$y_s/10^{-4}$	3.125±0.165	3.122	3.148
$y_b/10^{-2}$	1.639±0.015	1.639	1.637
$y_e/10^{-6}$	2.7947±0.02794	2.7945	2.7906
$y_\mu/10^{-4}$	5.8998±0.05899	5.9011	5.9080
$y_\tau/10^{-2}$	1.0029±0.01002	1.0022	1.0023
$\theta_{12}^{\rm CKM}/10^{-2}$	22.735±0.072	22.729 ($\theta_{12}^{\rm CKM}$ =13.023°)	22.730 ($\theta_{12}^{\rm CKM}$ =13.023°)
$\theta_{23}^{\rm CKM}/10^{-2}$	4.208±0.064	4.206 ($\theta_{23}^{\rm CKM}$ =2.401°)	4.204 ($\theta_{23}^{\rm CKM}$ =2.408°)
$\theta_{13}^{\rm CKM}/10^{-3}$	3.64±0.13	3.64 ($\theta_{13}^{\rm CKM}$ =0.208°)	3.64 ($\theta_{13}^{\rm CKM}$ =0.208°)
$\delta_{\rm CKM}$	1.208±0.054	1.209 ($\delta_{\rm CKM}$ =69.322°)	1.212 ($\delta_{\rm CKM}$ =69.457°)
$\Delta m_{21}^2/10^{-5}$	7.425±0.205	7.413	7.506
$\Delta m_{31}^2/10^{-3}$ (NO)	2.515±0.028	2.514	-
$\Delta m_{32}^2/10^{-3}$ (IO)	-2.498±0.028	-	-2.499
$\sin^2\theta_{12}$	0.3045±0.0125	0.3041 ($\theta_{12} = 33.46°$)	0.3067 ($\theta_{12} = 33.63°$)
$\sin^2\theta_{23}$ (NO)*	0.5705±0.0205	0.4473 ($\theta_{23} = 41.98°$)	-
$\sin^2\theta_{23}$ (IO)*	0.576±0.019	-	0.5784 ($\theta_{23} = 49.51°$)
$\sin^2\theta_{13}$ (NO)	0.02223±0.00065	0.02223 ($\theta_{13} = 8.57°$)	-
$\sin^2\theta_{13}$ (IO)	0.02239±0.00063	-	0.02238 ($\theta_{13} = 8.60°$)
$\delta_{\rm CP}^\circ$ (NO)	207.5±38.5	240.49	-
$\delta_{\rm CP}^\circ$ (IO)	284.5±29.5	-	263.49
$\eta_B/10^{-10}$	6.12±0.04‡	7.6 (7.6)	9.6 (51)
χ^2	-	1.45	5.76†

Table 1. Fitted values of the observables. See text for details. *Note that experimental measurements of θ_{23} have two local minima [73], one is for smaller and the other for larger values than 45°. For these experimental values, although only the best fit values from the global fit [73] are shown in this table, in the fitting procedure we have allowed the entire viable ranges. †For the inverted neutrino mass ordering, a significant contribution to χ^2, in particular, $(\Delta\chi^2)_{\theta_{23}} \approx 2.7$, originates from global fit to neutrino parameters [73]. ‡Since the uncertainty of the observed baryon asymmetry parameter η_B from Planck [88] is much smaller than the expected "theoretical uncertainty" alluded to in the previous section, we have not added its contribution to the total χ^2 quoted above (see text for more details). The generated η_B values quoted here are for zero (thermal) initial N_i abundance.

JHEP10(2024)190

We then perform a minimization of a χ^2-function at the $M_Z = 91.8176\,\mathrm{GeV}$ scale, which is defined as

$$\chi^2 = \sum_k \left(\frac{T_k - O_k}{E_k}\right)^2 , \tag{4.1}$$

where T_k, O_k, and E_k stand for theoretical prediction, experimentally observed central value, and 1σ experimental uncertainty, respectively, for the k-th physical quantity. The sum over k includes 3 up-type quark, 3 down-type quark, 3 charged lepton masses, 3 CKM (Cabibbo-Kobayashi-Maskawa) mixing angles, 1 Dirac phase in the CKM matrix, 2 neutrino mass-squared differences, 3 PMNS mixing angles, and 1 Dirac phase in the PMNS matrix. Low scale experimental values of these observables in the charged and neutral fermion sectors are taken from refs. [89] and [73, 90], respectively. The χ^2-function also includes the baryon asymmetry of the universe, η_B. Since the asymmetry is generated from the decay of the next-to-lightest right-handed neutrinos, η_B is computed using the Dirac Yukawa coupling Y_{ν_D} and the right-handed neutrino masses M_{ν_R} evaluated at M_2, the mass scale of N_2.

As pointed out first in ref. [50], this minimal Yukawa sector of SO(10) allows solutions for both normal ordering (NO) and inverted ordering (IO) of the light neutrino masses. In this work, we also consider these two scenarios and benchmark fit results are given in table 1. This table also includes the experimentally measured values of the observables and their associated 1σ uncertainties. Since the experiment errors on the charged fermion masses are very small, we have quoted 1% uncertainty in their masses in the table, which we have used. The fit parameters for these two cases (NO and IO) are provided in appendices A and B, respectively.

The right-handed neutrino mass spectra obtained from the best fits are

$$\mathrm{NO}: (M_1, M_2, M_3) = \left(6.57\times10^4, 2.08\times10^{12}, 8.10\times10^{14}\right)\ \mathrm{GeV}, \tag{4.2}$$

$$\mathrm{IO}: (M_1, M_2, M_3) = \left(1.06\times10^4, 1.72\times10^{12}, 5.85\times10^{14}\right)\ \mathrm{GeV}. \tag{4.3}$$

The light neutrino masses m_i, the effective neutrino mass appearing in neutrinoless double beta decay,[3] $m_{\beta\beta}$, and the Majorana phases α and β (cf. eq. (2.18)) are given as follows:

$$\mathrm{NO}: (m_1, m_2, m_3, m_{\beta\beta}) = (0.038, 8.61, 50.14, 3.68)\ \mathrm{meV},\ (\alpha,\beta) = (178.55^\circ, 124.46^\circ), \tag{4.4}$$

$$\mathrm{IO}: (m_1, m_2, m_3, m_{\beta\beta}) = (49.24, 49.99, 0.1923, 34.36)\ \mathrm{meV},\ (\alpha,\beta) = (100.76^\circ, 172.86^\circ). \tag{4.5}$$

Concerning the solutions presented in table 1, note that the total χ^2 per degrees of freedom for both the NO and IO solutions are similar. While the model admits both NO and IO spectra, global fits and cosmological constraints show a preference of NO over IO. A variation of the Dirac CP-violating phase, δ_{CP}, in the neutrino sector obtained for the case of normal ordering by marginalizing over all other model parameters is shown in figure 1. This plot shows a slight preference of the phase close to the region $\delta_{\mathrm{CP}} \in (230-300)^\circ$ for the solutions corresponding to $\theta_{23} < 45^\circ$ (the blue curve in figure 1). Although for NO,

[3] Note that heavy Majorana neutrinos can, in general, contribute to neutrinoless double beta decay. The current limits can be translated as $M_i \gtrsim 8.5\,\mathrm{TeV}|y_{i\alpha}|^{2/3}$ [91, 92]. However, our scenario is quite far from this limit: for the lightest one $M_1 \gtrsim 10^4$ GeV, we have $|y_{1\alpha}| \sim 10^{-6}$ while only for the heaviest one $M_3 \sim 10^{14}$ GeV, we have $|y_{3\alpha}| \sim 1$. Hence in all cases, their contributions are completely negligible.

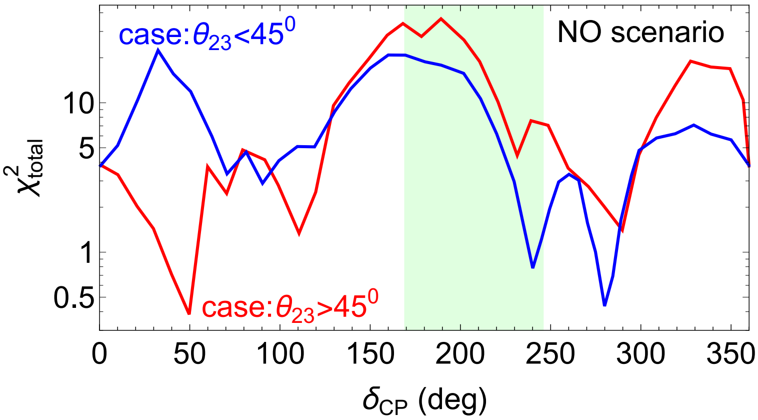

Figure 1. Variation of the Dirac CP-violating phase, $\delta_{\rm CP}$, in the neutrino sector obtained by marginalizing over all other model parameters for the case of NO solution. The 1σ range of $\delta_{\rm CP}$ from global fit is depicted with light green band [73]. For making this plot, in the numerical fit procedure, we have utilized analytical approximated formula for η_B, and demanded that the baryon asymmetry lies within the range $\eta_B/10^{-10} \in (5, 50)$. One should not get confused by the fact that at $\delta_{\rm CP} \sim 280^\circ$, one sees a deeper minimum compared to the solution presented in table 1. This is simply because the benchmark fit presented in table 1 is closer to the central value of $\delta_{\rm CP}$ obtained from global fit of neutrino observables. The blue (red) curve represents the solutions corresponding to the case $\theta_{23} < 45^\circ$ ($\theta_{23} > 45^\circ$).

solutions are also possible for the case of $\theta_{23} > 45^\circ$ (the red curve in figure 1), comparatively it has somewhat larger total χ^2 within the 1σ preferred range of $\delta_{\rm CP}$ from global fit (light green band in figure 1). In this particular case, the preferred value of the CP violating phase is rather close to $\delta_{\rm CP} \sim 50^\circ$.

For leptogenesis, the washout parameters defined in eq. (3.27) are obtained from the best fit and are given by

$$\text{NO}: \quad K_1(\mu = M_2) \simeq 19, \quad K_2(\mu = M_2) \simeq 0.39, \quad K_3(\mu = M_2) \simeq 63, \tag{4.6}$$

$$\text{IO}: \quad K_1(\mu = M_2) \simeq 70, \quad K_2(\mu = M_2) \simeq 0.65, \quad K_3(\mu = M_2) \simeq 88. \tag{4.7}$$

At $\mu = M_1$, while K_2 and K_3 remain the same, we have $K_1(\mu = M_1) \simeq 18$ and $K_1(\mu = M_1) \simeq 64$ for NO and IO, respectively. Notice that we found $M_3 \simeq 8 \times 10^{14}$ GeV and 5×10^{14} GeV for NO and IO, respectively. One could wonder whether for a sufficiently large reheat temperature, comparable to M_3, one should also include a contribution to the $B - L$ asymmetry from N_3-decays. However, we have checked that the $B - L$ asymmetry generated from N_3-decays is in any case negligible. This is because for $M_3 \gg M_2$ all N_3 *CP* flavored asymmetries are strongly suppressed. As for N_1, since $M_1 \ll 10^9$ GeV, the CP asymmetries are too small for leptogenesis, as one could expect from the usual Davidson-Ibarra lower bound on right-handed neutrino masses for successful leptogenesis [93]. Notice that since $K_1 \gg 1$, flavor effects are crucial to avoid the N_1 wash-out, since the wash-out suppression is exponential in K_1 [69, 70]. We will discuss this point in more detail in section 5. Finally, notice that since $M_2 \sim 10^{12}$ GeV and thanks to the interference with N_3, the N_2 decays can generate the correct asymmetry for successful leptogenesis. Since K_2 is close to the boundary between strong and weak washout regimes, one expects some sensitivity to the initial N_2 abundance.

JHEP10(2024)190

We indeed observe an order of magnitude enhancement in the asymmetry generation for the case of thermal initial N_2 abundance compared to the case of initial vanishing N_2 abundance at the production. This is because in this case the small neutrino Yukawa interactions are not responsible for the production of the N_2 abundance that is assumed to be thermal prior to N_2 decays. This should not be regarded as a drawback of the scenario since the thermalisation of the N_2 abundance can be achieved thanks to the SO(10) gauge interactions, as we previously discussed, if the reheat temperature is sufficiently large (see eq. (3.12)).

Solving the Boltzmann equations discussed in section 3, the resulting values of baryon to photon number density today assuming zero (thermal) initial N_i abundances are found for the best fit to be

$$\text{NO} : \eta_B = 7.6\,(7.6) \times 10^{-10}, \qquad \text{IO} : \eta_B = 9.6\,(51) \times 10^{-10}, \tag{4.8}$$

which are slightly larger than the observed value $(6.12 \pm 0.04) \times 10^{-10}$ [88]. Due to the "theoretical uncertainty" mentioned at the end of the previous section, we have not included this measurement into the fit. Instead, we just require the generated asymmetry to be of the correct sign and not smaller than the observed value.[4] Though we did observe enhanced asymmetry generation from N_2 leptogenesis with thermal initial N_2 abundance for both NO and IO cases, curiously, nontrivial flavor effects during N_1 washout renders the final asymmetry to be the same as that of zero initial N_2 abundance in the NO case while some enhancement survives for the IO case. What we observe in the *charged lepton flavor basis* where y_E is diagonal is the following. The N_1 washout of the initially dominant $(Y_{\tilde{\Delta}} - Y_{\Delta E})_{\tau\tau}$ (from N_2 leptogenesis) is strong for both NO and IO scenarios, which makes it eventually subdominant. On the other hand, the N_1 washout of $(Y_{\tilde{\Delta}} - Y_{\Delta E})_{\mu\mu}$ is under control for both NO and IO scenarios, eventually making it the dominant one with positive sign. Finally, the N_1 washout of $(Y_{\tilde{\Delta}} - Y_{\Delta E})_{ee}$ is weak and strong in the NO and IO scenarios, respectively, making it relevant only for the NO scenario. Due to the negative sign in the final $(Y_{\tilde{\Delta}} - Y_{\Delta E})_{ee}$, it partially cancels $(Y_{\tilde{\Delta}} - Y_{\Delta E})_{\mu\mu}$ in the NO scenario such that the final asymmetry in both zero and thermal N_i remains similar. This is another example of the importance of flavor effects in leptogenesis. In section 5 we will provide some analytical insight on these results on the final asymmetry, showing how flavor effects can explain it.

4.2 Features of the minimal Yukawa sector

In the following, we illustrate two unique features of the minimal Yukawa sector, namely (i) the right-handed neutrino spectrum is predicted and (ii) contrary to other SO(10) setups, inverted neutrino mass ordering solution is possible within this framework. First, one important feature of this model is that, a viable fit to fermion mass spectrum can obtained provided that 2×10^{13} GeV $\lesssim M_3 \lesssim 10^{15}$ GeV [50], while best fit typically prefers $M_3 \sim 10^{14}$ GeV. Moreover, for the moment, focusing only on orders of the diagonal entries (hence antisymmetric contribution is ignored), the up-type quark, down-type quark, and charged lepton mass

[4]While a larger baryon asymmetry can always be reduced by additional entropy injection and/or washout processes after baryogenesis, a scenario which generates an insufficient asymmetry is a failed baryogenesis by definition.

matrices are,

$$M_U \sim D + S, \qquad M_D \sim D + r_1 S, \qquad M_E \sim D - 3r_1 S. \tag{4.9}$$

It is obvious from these relations that the only consistent solution can be found if $D \ll S$ and $r_1 \ll 1$. One, therefore, has $D_{33} + r_1 S_{33} \sim m_b$ (and similarly, $D_{33} - 3r_1 S_{33} \sim m_\tau$), whereas $S_{33} \sim m_t$ (for the top quark mass, D_{33} plays no role owing to its smallness). Due to the smallness of strange-quark mass compared to the charm-quark mass, a similar argument is also valid for the second generation (however, such an argument is not applicable to the first generation). Therefore, reproducing the correct fermion mass hierarchies demands,

$$S \sim \begin{pmatrix} S_{11} & & \\ & m_c & \\ & & m_t \end{pmatrix}. \tag{4.10}$$

Then the ratio r_1 must obey $r_1 \lesssim 10^{-2}$ not to provide too large contributions to the masses in the down-type quark sector. An immediate consequent is that

$$M_2 \sim \frac{m_c}{m_t} M_3 \sim 10^{11-12}\ \text{GeV}, \tag{4.11}$$

which is a prediction of this scenario. The features mentioned above are true for both NO and IO solutions.

Furthermore, the S_{11} entry plays no role in charged fermion mass fit, which is solely fixed by the requirement of reproducing correct neutrino fit. Looking at the light neutrino mass matrix at the GUT scale and using the fit parameters, we obtain (for illustration, we only present the order of the numbers)

$$m_\nu = -M_{\nu_D}^T \begin{pmatrix} M_1^{-1} & & \\ & M_2^{-1} & \\ & & M_3^{-1} \end{pmatrix} M_{\nu_D}, \tag{4.12}$$

$$\sim \begin{pmatrix} \frac{3\times10^{-7}}{M_1} + 10^{-17} & \frac{4\times10^{-7}}{M_1} + 10^{-15} & \frac{4\times10^{-7}}{M_1} + 10^{-15} \\ & \frac{4\times10^{-7}}{M_1} + 10^{-13} & \frac{6\times10^{-7}}{M_1} + 10^{-13} \\ & & \frac{6\times10^{-7}}{M_1} + 10^{-10} \end{pmatrix}_{\text{NO}}, \tag{4.13}$$

$$\xrightarrow{M_1^{\text{NO}} \sim 10^5\ \text{GeV}} \begin{pmatrix} 5\times10^{-12} & 6\times10^{-12} & 6\times10^{-12} \\ & 9\times10^{-12} & 9\times10^{-12} \\ & & 8\times10^{-11} \end{pmatrix}_{\text{NO}}. \tag{4.14}$$

The contributions from $M_{2,3}$ are presented in gray. It turns out that apart from the (3,3) entry, contributions from M_3 are completely negligible. However, subleading contributions from M_2 on the (2,2), and (2,3) entries cannot be fully ignored. For the rest of the terms, M_1 contributions dominate over the rest. Hence, the mass of the lightest right-handed neutrino, M_1, plays a vital role in generating neutrino masses via type-I seesaw formula. Therefore, M_1 cannot be larger than a certain value. To provide sufficient contributions and reproduce neutrino oscillation data, for the NO solution, one must have $M_1^{\text{NO}} \sim 10^5$ GeV. This accordingly fixes $S_{11} \sim 10^{-9}$, making it irrelevant for charged fermion masses.

On the other hand, for IO case, $M_1^{\rm IO}$ must be about an order of magnitude smaller than $M_1^{\rm NO}$ such that it provides dominant contributions in the first row and first column of m_ν. In particular, using the fit parameters, we find (as before, we only present the order of the numbers)

$$m_\nu \sim \begin{pmatrix} \frac{5\times10^{-7}}{M_1} + 10^{-17} & \frac{7\times10^{-8}}{M_1} + 10^{-15} & \frac{4\times10^{-7}}{M_1} + 10^{-15} \\ & \frac{10^{-8}}{M_1} + 10^{-13} & \frac{6\times10^{-8}}{M_1} + 10^{-13} \\ & & \frac{3\times10^{-7}}{M_1} + 10^{-10} \end{pmatrix}_{\rm IO} , \tag{4.15}$$

$$\xrightarrow{M_1^{\rm IO}\sim 10^4\ {\rm GeV}} \begin{pmatrix} 5\times10^{-11} & 8\times10^{-12} & 4\times10^{-11} \\ & 10^{-12} & 6\times10^{-12} \\ & & 3\times10^{-11} \end{pmatrix}_{\rm IO} . \tag{4.16}$$

This shows that the model predicts $M_1 \sim 10^5\,\text{GeV}$ for NO and $M_1 \sim 10^4\,\text{GeV}$ for IO. Summarizing, the model predicts,

$$(M_1, M_2, M_3) \sim \left(10^{4-5}, 10^{11-12}, 10^{14-15}\right)\ \text{GeV}. \tag{4.17}$$

It is intriguing to point out that such a high value $\sim 10^{15}\,\text{GeV}$ of the $B-L$ symmetry breaking scale could explain the recently observed gravitational waves at nanoHertz frequencies (see, for example, ref. [94]). A series of pulsar timing arrays, CPTA [95], EPTA [96], NANOGrav [97], and PPTA [98], very recently reported this result, which could originate from metastable cosmic strings with a string tension, $\mu_{\rm cs}$, such that $G\mu_{\rm cs} \sim 10^{-7}$ [99] (here, G is the Newton's constant, and, $G\mu_{\rm cs}$ is the dimensionless string tension parameter), corresponding to a metastable cosmic string network formation scale of $\sim 10^{15}\,\text{GeV}$.

5 Comparison with SO(10)-inspired leptogenesis

In this section we compare the obtained numerical results with the analytical results obtained within the framework of SO(10)-inspired leptogenesis [64, 66, 68]. First of all, it is convenient to define the quantities $N_X \equiv Y_X/Y_{N_2}^{\rm eq}(T \gg M_2)$, so that simply $N_{N_2}^{\rm eq}(T \gg M_2) = 1$. The final $B-L$ asymmetry has to be calculated as the sum of the three charged lepton flavor asymmetries

$$N_{B-L}^{\rm f} = \sum_{\alpha=e,\mu,\tau} N_{\Delta_\alpha} , \tag{5.1}$$

where $\Delta_\alpha \equiv B/3 - L_\alpha$. The baryon-to-photon ratio predicted by leptogenesis can then be calculated as $0.96\times10^{-2}\,N_{B-L}^{\rm f}$. We also define the neutrino Dirac mass matrix in the charged lepton mass basis as $m_D \equiv (M_{\nu_D} E_L)^\dagger$ and define the corresponding light neutrino mass matrix in the flavor basis as $\bar{m}_\nu \equiv -m_D M^{-1} m_D^T$ in a way that, in terms of $\bar{m}_\nu$, the light neutrino Majorana mass term is $\overline{\nu}\,\bar{m}_\nu\,\nu^c/2$ with mass eigenvalues $D_m \equiv {\rm diag}(m_1, m_2, m_3)$. Within SO(10)-inspired leptogenesis it is assumed that if one diagonalises the neutrino Dirac mass matrix with a biunitary transformation, $m_D =$

$V_L^\dagger {\rm diag}(m_{D1}, m_{D2}, m_{D3})\, U_R$, then $(m_{D1}, m_{D2}, m_{D3}) \simeq (m_u, m_c, m_t)$ and $V_L \simeq U_{\rm CKM}$ [55–60].

The spectrum of right-handed neutrino masses resulting from the seesaw formula in combination with the low energy neutrino experimental data is very hierarchical with

$M_1 \ll 10^9\,\mathrm{GeV}$ and $M_2 \sim 10^{11}$–$10^{12}\,\mathrm{GeV}$, exactly of the kind obtained in the numerical fit. With such a hierarchical spectrum, the neutrino Dirac mass eigenvalue that enters the final asymmetry is $m_{D2} \sim m_c$, while m_{D1} and m_{D3} cancel out and do not play any role: for this reason there is a reduction of the number of parameters that determines the asymmetry and once the condition of successful leptogenesis is imposed, there are some interesting constraints on low energy neutrino parameters. From this point of view the numerical fit that we have obtained seems to respect the main features of the solutions obtained in SO(10)-inspired leptogenesis. In particular, NO solutions are favoured and first octant for θ_{23} is also favoured. There is, however, one remarkable departure from the solutions obtained within SO(10)-inspired leptogenesis. The final asymmetry is either tauon dominated, with $N^{\mathrm{f}}_{B-L} \simeq N_{\Delta_\tau}$, or muon dominated, with $N^{\mathrm{f}}_{B-L} \simeq N_{\Delta_\mu}$. In both cases one obtains a lower bound on the absolute neutrino mass scale that in terms of lightest neutrino mass can be expressed as $m_1 \gtrsim 1\,\mathrm{meV}$ in the case of tauon-dominated solutions and $m_1 \gtrsim 20\,\mathrm{meV}$ in the case of muon-dominated solutions, where we refer to the, by far more interesting, NO case.

In the numerical fit we have obtained, the asymmetry is muon-dominated but as one can see one has $m_1 \simeq 0.038\,\mathrm{meV}$, violating the lower bound obtained for SO(10)-inspired leptogenesis with $V_L \simeq U_{\mathrm{CKM}}$. If we parameterise the unitary matrix V_L in terms of three mixing angles and six phases, we can write:

$$V_L = \begin{pmatrix} c^L_{12}\,c^L_{13} & s^L_{12}\,c^L_{13} & s^L_{13}\,e^{-\mathrm{i}\,\delta_L} \\ -s^L_{12}\,c^L_{23} - c^L_{12}\,s^L_{23}\,s^L_{13}\,e^{\mathrm{i}\,\delta_L} & c^L_{12}\,c^L_{23} - s^L_{12}\,s^L_{23}\,s^L_{13}\,e^{\mathrm{i}\,\delta_L} & s^L_{23}\,c^L_{13} \\ s^L_{12}\,s^L_{23} - c^L_{12}\,c^L_{23}\,s^L_{13}\,e^{\mathrm{i}\,\delta_L} & -c^L_{12}\,s^L_{23} - s^L_{12}\,c^L_{23}\,s^L_{13}\,e^{\mathrm{i}\,\delta_L} & c^L_{23}\,c^L_{13} \end{pmatrix} \times \mathrm{diag}\left(e^{-i\,\frac{\alpha_L}{2}}, e^{-i\,\frac{\beta_L}{2}}, 1\right), \tag{5.2}$$

where $c^L_{ij} = \cos\theta^L_{ij}$ and $s^L_{ij} = \sin\theta^L_{ij}$. We have extracted this matrix in the case of the best numerical fit and found that while $\theta^L_{12} \simeq 4^\circ$ and $\theta^L_{13} \simeq 0.3^\circ$ respect the condition to be comparable to the corresponding values of the angles in the CKM matrix, one has $\theta^L_{23} \simeq 45^\circ$, a maximal value corresponding to a drastic departure from the condition $V_L \simeq U_{\mathrm{CKM}}$. It was already noticed that a non-vanishing value of θ^L_{23} is necessary to have non-vanishing $\varepsilon_{2\mu}$ and, therefore, muon dominated solutions [66]. However, this angle was still kept small and it was shown one could not obtain successful leptogenesis in the normal hierarchical limit ($m_1 \ll m_{\mathrm{sol}} \equiv \sqrt{\Delta m^2_{21}} \sim 10\,\mathrm{meV}$). Here we want to show how, thanks to a large value of θ^L_{23}, one can have successful (muon dominated) leptogenesis with m_1 as small as $0.038\,\mathrm{meV}$, as obtained in the numerical fit.

If in first approximation we neglect flavor coupling stemming from spectator processes, mainly dominated by the Higgs asymmetry, an analytical expression for the muonic contribution is given by

$$N^{\mathrm{lep,f}}_{\Delta_\mu} \simeq \varepsilon_{2\mu}\,\kappa(K_{2e}+K_{2\mu})\,e^{-\frac{3\pi}{8}\,K_{1\mu}}\,, \tag{5.3}$$

where $K_{1\mu}$, $K_{2\mu}$ and K_{2e} are the flavored decay parameters given by $K_{i\alpha} = |(m_D)_{\alpha i}|^2/(M_i\,m_\star)$, $\varepsilon_{2\mu}$ is the muonic CP asymmetry and $\kappa(K_{2e}+K_{2\mu})$ is the efficiency factor at the production, i.e., at the scale M_2. For initial thermal N_2 abundance this can be calculated as

$$\kappa(K_{2\alpha}) = \frac{2}{z_B(K_{2e}+K_{2\mu})\,(K_{2e}+K_{2\mu})}\left(1 - e^{-\frac{(K_{2e}+K_{2\mu})\,z_B(K_{2e}+K_{2\mu})}{2}}\right), \tag{5.4}$$

with

$$z_B(K_{2e}+K_{2\mu}) \simeq 2 + 4\,(K_{2e}+K_{2\mu})^{0.13}\,e^{-\frac{2.5}{K_{2e}+K_{2\mu}}}\,. \tag{5.5}$$

We have now to understand the effect of a maximal $\theta^L_{23} = 45°$. For simplicity we can approximate $\theta^L_{12} \simeq \theta^L_{13} \simeq 0$. A very useful quantity in connecting the neutrino Dirac mass matrix to the low energy neutrino parameters via the seesaw formula when $V_L \neq I$ is the neutrino mass matrix in the Yukawa basis given by $\widetilde{m}_\nu = V_L\,\bar{m}_\nu\,V_L^T$, that is clearly symmetric. In particular, the right-handed neutrino masses can be expressed in a compact way in terms of the $\widetilde{m}_\nu$ entries as:

$$M_1 \simeq \frac{m^2_{D1}}{|(\widetilde{m}_\nu)_{11}|}\,, \qquad M_2 \simeq \frac{m^2_{D2}}{m_1\,m_2\,m_3}\,\frac{|(\widetilde{m}_\nu)_{11}|}{|(\widetilde{m}_\nu^{-1})_{33}|}\,, \qquad M_3 \simeq m^2_{D3}\,|(\widetilde{m}_\nu^{-1})_{33}|\,. \tag{5.6}$$

Since we take only θ^L_{23} large, it is easy to see that the only entries $(\widetilde{m}_\nu)_{ij}$ that change compared to the case $V_L = I$ are $(\widetilde{m}_\nu)_{23}$ and $(\widetilde{m}_\nu)_{33}$. With this observation it is simple to see the effect of having a large θ^L_{23} in the muon-dominated final asymmetry.

Let us start from calculating $K_{1\mu}$. It is simple to derive the following approximate expression in the hierarchical limit ($m_1 \ll m_{\rm sol}$) [66]:

$$K_{1\mu} = \frac{|(m_D)_{\mu 1}|^2}{M_1\,m_\star} \simeq c^2_{12}\,c^2_{23}\,\frac{m_{\rm sol}}{m_\star} \simeq 3\,. \tag{5.7}$$

In this expression we have neglected a correcting term $(s^L_{23})^2\,|(\widetilde{m}_\nu)_{13}|^2/(|(\widetilde{m}_\nu)_{11}|m_\star)$, so that there is no substantial change in $K_{1\mu}$ even with a maximal value $\theta^L_{23} = 45°$. Notice that this result implies that there is necessarily a suppression of the muon asymmetry produced from N_2 decays due to the N_1 washout given by a factor $e^{-3\pi\,K_{1\mu}/8} \simeq 0.03$. This suppression of course needs to be compensated mainly by a large enhancement of the muonic *CP* asymmetry $\varepsilon_{2\mu}$ and, to a minor extent, by a small value of $K_{2e}+K_{2\mu}$ so that $\kappa(K_{2e}+K_{2\mu}) \simeq 1$ for initial thermal N_2 abundance.

Let us show that this is indeed what happens starting from the crucial quantity $\varepsilon_{2\mu}$. An approximate expression for $\varepsilon_{2\mu}$ is given by

$$\varepsilon_{2\mu} \simeq \frac{3}{16\,\pi}\,\frac{M_2}{M_3}\,\frac{{\rm Im}\left[(m_D)^\star_{\alpha 2}(m_D)_{\alpha 3}(m_D^\dagger\,m_D)_{23}\right]}{v^2\,(m_D^\dagger\,m_D)_{22}}\,. \tag{5.8}$$

From this expression, using the eqs. (5.6) for M_2 and M_3, the biunitary parameterisation for $m_{\rm D}$ and an expression of U_R in terms of $\widetilde{m}_\nu$ entries, one arrives to the following approximate expression for $\varepsilon_{2\mu}$:

$$\varepsilon_{2\mu} \simeq \frac{3\,m^2_{D2}}{16\,\pi\,v^2}\,\frac{|(\widetilde{m}_\nu)_{11}|\,|(V_L)_{32}|^2}{m_1\,m_2\,m_3\,|(\widetilde{m}_\nu^{-1})_{33}|^2}\,\sin\alpha_{\rm lep}\,, \tag{5.9}$$

where from eq. (5.2) one can see that, in our case, $|(V_L)_{32}|^2 = (s^L_{23})^2 \sim 1$. Moreover, one finds for the effective phase

$$\alpha_{\rm lep} = {\rm Arg}\,[(\widetilde{m}_\nu)_{11}] - 2\,{\rm Arg}[(\widetilde{m}_\nu^{-1})_{23}] - \pi + \alpha - 2\,\beta + \alpha_L - 2\,\beta_L\,. \tag{5.10}$$

It should be immediately noticed how the *CP* asymmetry vanishes in the limit $\theta^L_{23} \to 0$ showing how muon-dominated solutions necessarily require some departure from the case

$V_L = I$. We now have to understand how one can have an enhancement in the hierarchical limit, for $m_1 \ll m_{\rm sol}$. The crucial point is to have a small value of $|(\widetilde{m}_\nu^{-1})_{33}|$. Let us calculate this important quantity. First of all notice that $\widetilde{m}_\nu^{-1} = V_L^\star \, \bar{m}_\nu^{-1} \, V_L^\dagger$ so that one obtains

$$(\widetilde{m}_\nu^{-1})_{33} = (V_L^\star)^2_{33} \, (\bar{m}_\nu^{-1})_{33} + (V_L^\star)^2_{32} \, (\bar{m}_\nu^{-1})_{22} + 2 \, (V_L^\star)_{32} (V_L^\star)_{33} \, (\bar{m}_\nu^{-1})_{23} \, . \tag{5.11}$$

The inverse low energy neutrino mass matrix is given by $\bar{m}_\nu^{-1} = U_\nu^\star \, D_{\rm m}^{-1} \, U_\nu^\dagger$, so that one finds in the hierarchical limit:

$$(\bar{m}_\nu^{-1})_{33} \simeq \frac{s_{12}^2 s_{23}^2}{m_1} \, e^{i\alpha} \, , \qquad (\bar{m}_\nu^{-1})_{22} \simeq \frac{s_{12}^2 \, c_{23}^2}{m_1} \, e^{i\alpha} \, , \qquad (\bar{m}_\nu^{-1})_{23} \simeq -\frac{s_{12}^2 \, s_{23} \, c_{23}}{m_1} \, e^{i\alpha} \, . \tag{5.12}$$

Notice that for $m_1 \to 0$, one has $(\widetilde{m}_\nu^{-1})_{33} \propto 1/m_1$ implying $\varepsilon_{2\mu} \propto m_1 \to 0$. It is then necessary that the factor of proportionality $(\widetilde{m}_\nu^{-1})_{33} \, m_1$ gets sufficiently small in order to have successful leptogenesis. This also corresponds to have a reduction of the ratio $M_2/M_3 \propto (\widetilde{m}_\nu^{-1})^2_{33}$. This implies that there must be some phase cancellation. Let us see whether this is possible for some choice of the values of some of the phases.

In the hierarchical limit one obtains then the following expression for $(\widetilde{m}_\nu^{-1})_{33}$:

$$(\widetilde{m}_\nu^{-1})_{33} \, m_1 \simeq s_{12}^2 \, e^{i\alpha} \left[(c_{23}^L)^2 \, s_{23}^2 + 2 s_{23}^L \, c_{23}^L s_{23} c_{23} \, e^{i \frac{\beta_L}{2}} + (s_{23}^L)^2 \, c_{23}^2 \, e^{i\beta_L} \right] . \tag{5.13}$$

For $\theta_{23}^L = \pi/4$, one has a cancellation in the second term if $\beta_L \simeq 2n\,\pi$ with n integer number in a way that one obtains

$$|(\widetilde{m}_\nu^{-1})_{33}| \, m_1 \simeq \frac{s_{12}^2}{2} (c_{23} - s_{23})^2 \sim 0.01 \, , \tag{5.14}$$

where for the numerical estimation we used the best fit values for θ_{12} and θ_{23}. Notice that in our fit we indeed find $\beta_L \simeq -2\pi$ and $|(\widetilde{m}_\nu^{-1})_{33}| \, m_1 \sim 0.01$, in nice agreement with this analytical result. The smallness of $|(\widetilde{m}_\nu^{-1})_{33}| \, m_1$, combined with a large $\theta_{23}^L \simeq \pi/4$, strongly enhances the muonic CP asymmetry, allowing successful leptogenesis despite that for $m_1 \ll m_{\rm sol}$ one has $K_{1\mu} \simeq 3$, as we have seen. Notice that a small $|(\widetilde{m}_\nu^{-1})_{33}|$ is also important to suppress $K_{2e} + K_{2\mu}$ since one has in the hierarchical limit

$$K_{2\mu} = \frac{|(m_D)_{\mu 2}|^2}{M_2 \, m_\star} \simeq (c_{23}^L)^2 \, \frac{m_1 \, m_{\rm sol} \, m_{\rm atm}}{m_\star \, |(\widetilde{m}_\nu)_{11}|} \, |(\widetilde{m}_\nu^{-1})_{33}| \sim 0.1 \, , \tag{5.15}$$

and $K_{2e} \ll K_{2\mu}$. It is interesting that the value θ_{23}^L seems to be a special one in order to have such phase cancellation and this might suggest the presence of some discrete symmetry. It is also interesting that in this case the deviation of the atmospheric mixing angle from the maximal value sets the value of $|(\widetilde{m}_\nu^{-1})_{33}| \, m_1$ and, consequently, of the baryon asymmetry.[5]

Finally, let us say that an analogous result holds for inverted ordering, though this possibility is now strongly disfavoured by recent results from neutrino oscillation experiments [100] and new cosmological observations placing a very stringent upper bound on the sum of neutrino masses [101].

[5]Notice that for $\theta_{23} = \pi/4$ one would have an exact cancellation and $(\widetilde{m}_\nu^{-1})_{33} = 0$ (in this case the validity of eqs. (5.6) breaks down). This would correspond to one of the two so-called crossing level solutions (the second is realised for $(\widetilde{m}_\nu)_{11} = 0$ and in that case one has $M_1 = M_2$) studied in [59] for small mixing angles in V_L. Therefore, the fit we found is just in the vicinity of the crossing level solution $(\widetilde{m}_\nu^{-1})_{33} = 0$ (corresponding to $M_2 = M_3$).

6 Gauge coupling unification and proton decay

Proton decay is the smoking gun signal of grand unification. For a recent review on this subject, see, for example, ref. [102]. In the framework of non-supersymmetric SO(10) GUTs, the most significant proton decay mode is the $p \to e^+\pi^0$ and the corresponding lifetime of the proton can be estimated as follows [103, 104]:

$$\tau_p = \Bigg[g_{\rm GUT}^4 \frac{m_p}{32\pi} \left(1 - \frac{m_{\pi^0}^2}{m_p^2}\right)^2 A_L^2 \times \\ \left\{ A_{SR}^2 \left(\frac{M_{X,Y}^2 + M_{X',Y'}^2}{M_{X,Y}^2 M_{X',Y'}^2}\right)^2 \left|\langle \pi^0 | (ud)_R u_L | p\rangle\right|^2 + A_{SL}^2 \frac{4}{M_{X,Y}^4} \left|\langle \pi^0 | (ud)_L u_L | p\rangle\right|^2 \right\} \Bigg]^{-1}. \tag{6.1}$$

Here, m_p and $g_{\rm GUT}$ represent the proton mass and the unified gauge coupling, respectively. $M_{X,Y}$ and $M_{X',Y'}$ denote the masses of the gauge bosons $X, Y \in (3, 2, 5/6)$ and $X', Y' \in (3, 2, -1/6)$. For our analysis, we identify the scale at which all gauge couplings unify, the GUT scale, with these gauge boson masses. Although the masses $M_{X,Y}$ and $M_{X',Y'}$ are in general different, they are nearly degenerate in the symmetry breaking scheme that we adopt here with an intermediate Pati-Salam symmetry, as they belong to the same $(6, 2, 2)$ multiplet of the PS symmetry.

The values of the hadronic matrix elements appearing in eq. (6.1) have been computed on the lattice and are found to be $\langle \pi^0 | (ud)_R u_L | p\rangle = -0.131\,\text{GeV}^2$ and $\langle \pi^0 | (ud)_L u_L | p\rangle = 0.134\,\text{GeV}^2$ [105]. Furthermore, the long-distant renormalization group running factor A_L [106] has a value given by $A_L \approx 1.2$, and the short range renormalization factor A_S is computed as follows [107–110]:

$$A_S = \prod_j^{M_Z \le M_j \le M_X} \prod_i \left[\frac{\alpha_i\,(M_{j+1})}{\alpha_i\,(M_j)}\right]^{\frac{\gamma_i}{b_i}}, \tag{6.2}$$

where, the beta function coefficients b_i are explicitly presented later in this section. Furthermore, $\alpha_i = g_i^2/4\pi$ and γ_i's are the relevant anomalous dimensions [111]. Values of the anomalous dimensions to be used for our numerical studies are [112–114]: for the SM gauge group, $\gamma^L_{3C,2L,1Y} = \{2, \frac{9}{4}, \frac{23}{20}\}$ and $\gamma^R_{3C,2L,1Y} = \{2, \frac{9}{4}, \frac{11}{20}\}$; whereas, for the Pati-Salam intermediate gauge group with parity we have $\gamma^L_{4C,2L,2R} = \gamma^R_{4C,2L,2R} = \{\frac{15}{4}, \frac{9}{4}, \frac{9}{4}\}$.

In order to satisfy the current proton lifetime bound of $\tau_p(p \to e^+\pi^0) > 2.4 \times 10^{34}$ yrs from Super-Kamiokande [87], one requires the GUT scale to be $M_{\rm GUT} \gtrsim 5 \times 10^{15}$ GeV. This limit follows from eq. (6.1) when the values of the various parameters appearing in it are inserted as discussed above. In the following we show how this limit can be respected in our scenario while also being consistent with gauge coupling unification. For this purpose a symmetry breaking scheme should be specified with the intermediate scale gauge symmetry identified. The scalar spectrum that survive below the GUT scale down to the intermediate scale ($M_{\rm int}$) should also be specified. For this we shall adopt a minimal scenario dictated by the extended survival hypothesis [115–118]. Under this hypothesis, only those scalar fragments from the GUT multiplets needed for subsequent symmetry breaking are assumed to survive down to the intermediate scale.

As discussed in section 4, the heaviest right-handed neutrinoN_3 has a mass of 2×10^{13} GeV $\lesssim M_{N_3} \lesssim 10^{15}$ GeV. This follows solely from the fermion fit [50]. Since N_3

JHEP10(2024)190

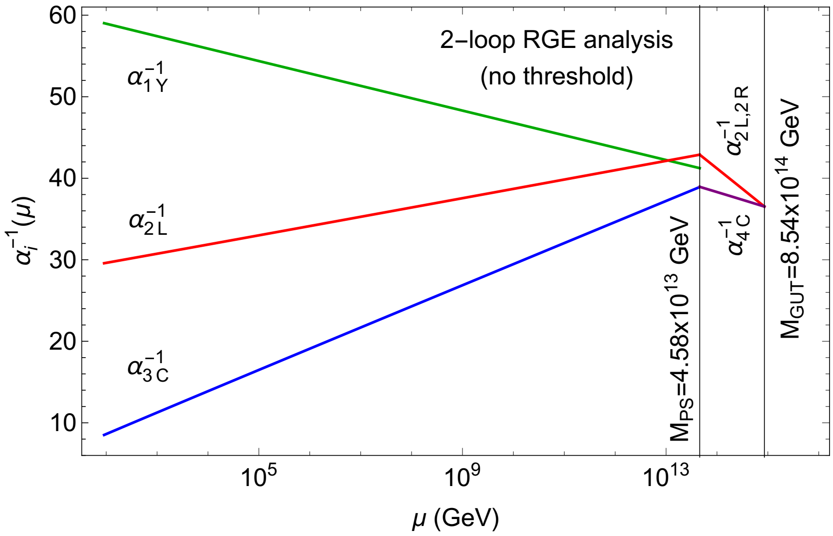

Figure 2. Gauge coupling evolution with an intermediate $SU(4)_c \times SU(2)_L \times SU(2)_R$ symmetry and an unbroken Z_2 parity. The minimal set of particle content affecting the running above the intermediate scale is $(1,2,2)_\mathcal{R} \subset 10_H$, $(1,2,2)_\mathcal{R}, (15,2,2)_\mathcal{R} \subset 120_H$, and $(1,2,2), (15,2,2), (10,1,3), (\overline{10},3,1) \subset \overline{126}_H$. Here, for clarity, real representations are denoted by a subscript $\mathcal{R}$. No threshold effects are included here. All particles surviving to $M_{\rm int}$ are taken to be degenerate, and all particles at the GUT scale are also taken to be degenerate.

mass can only arise after intermediate symmetry breaking, and since the relevant Yukawa coupling should be not more than order unity (so that perturbative unitarity is preserved), we infer that $(2-4) \times 10^{13}$ GeV $\lesssim M_{\rm int}$. Furthermore, the best fit for the fermion spectrum typically prefers this scale to be $M_{N_3} \sim (1-10) \times 10^{14}$ GeV, which suggests that $M_{\rm int}$ should be also in this range. Remarkably, preference of such a high intermediate scale ($M_{\rm int}$) points towards a particular symmetry breaking scheme, viz., where SO(10) breaks down to the $SU(4)_c \times SU(2)_L \times SU(2)_R$ Pati-Salam subgroup with an unbroken Z_2 parity. To be specific, with the assumption of extended survival hypothesis, in ref. [43], two schemes of SO(10) symmetry breaking was analyzed. If a 54_H is used for the GUT symmetry breaking, gauge coupling unification requires $M_{\rm int}$ to be about two orders of magnitude below $M_{\rm GUT}$ (from 1-loop RGE analysis). This is fully consistent with the above-mentioned range of 2×10^{13} GeV $\lesssim M_{\rm int} \lesssim 10^{15}$ GeV. However, if a 45_H or 210_H is used for the GUT breaking, SO(10) would break down to the Pati-Salam symmetry, but without the Z_2 parity, in which case $M_{\rm int} \simeq 10^{11}$ GeV would follow [43] (from 1-loop RGE analysis). The fermion mass fit to the minimal Yukawa sector that we have adopted here, therefore, prefers the GUT symmetry breaking Higgs to be in the 54-dimensional representation.

Therefore, for consistency, in this work, we consider the following symmetry breaking chain:

$$\mathrm{SO}(10) \xrightarrow[54_H]{M_{\rm GUT}} \mathrm{SU}(4)_C \times \mathrm{SU}(2)_L \times \mathrm{SU}(2)_R \times D \tag{6.3}$$

$$\xrightarrow[126_H]{M_{\rm int}} \mathrm{SU}(3)_C \times \mathrm{SU}(2)_L \times \mathrm{U}(1)_Y \tag{6.4}$$

$$\xrightarrow[10_H+120_H+126_H]{M_{EW}} \mathrm{SU}(3)_C \times \mathrm{U}(1)_{\rm em} \tag{6.5}$$

such that $M_{\rm GUT} > M_{\rm int} > M_{EW}$. As mentioned earlier, $M_{\rm GUT}$ is identified with the mass of the $M_{X^{(\prime)},Y^{(\prime)}}$ gauge bosons. Similarly, we identify $M_{\rm int}$ with the mass of leptoquark gauge boson of the Pati-Salam symmetry, $V_\mu(\overline{3},1,-2/3)$. The rest of the gauge bosons at $M_{\rm int}$ are not, however, degenerate with M_V, with their masses given by the relations $m_{W_R}/M_{\rm int} = g_{2R}/g_{4C}$ and $m_{Z_R}/M_{\rm int} = (3/2 + g_{2R}^2/g_{4C}^2)^{1/2}$ [119]. We shall take account of this non-degeneracy in the calculation of gauge coupling evolution.

Thus, GUT symmetry is first spontaneously broken to the Pati-Salam symmetry with a discrete Z_2 symmetry D, which is subsequently broken down to the SM when $\overline{126}_H$ acquires a VEV of order $M_{\rm int}$. This discrete symmetry guarantees that $g_{2L,\rm PS} = g_{2R,\rm PS}$. This symmetry breaking is also responsible for generating the mass of the heavy right-handed neutrinos. Hereafter, with this symmetry breaking chain, we perform a detailed analysis of the gauge coupling unification. The 2-loop RGEs for the gauge couplings g_i $(i = 1, 2, 3)$ are given by

$$\frac{d\alpha_i^{-1}(\mu)}{d\ln\mu} = -\frac{b_i}{2\pi} - \sum_j \frac{b_{ij}}{8\pi^2\alpha_j^{-1}(\mu)}, \tag{6.6}$$

where μ denotes the energy scale. At the low scale, i.e., $\mu = M_Z$, we use the following values of the gauge coupling [89]:

$$g_1(M_Z) = 0.461425^{+0.000044}_{-0.000043},\ g_2(M_Z) = 0.65184^{+0.00018}_{-0.00017},\ g_3(M_Z) = 1.2143^{+0.0036}_{-0.0035}. \tag{6.7}$$

Using the generalized formula for the beta-function, $\beta = \mu dg/d\mu$, the 1-loop and 2-loop coefficients are given by [120]

$$b_i = -\frac{11}{3}C_2(G_i) + \frac{4}{3}\kappa S_2(F_i) + \frac{1}{6}\eta S_2(S_i), \tag{6.8}$$

$$\begin{aligned} b_{ij} = &-\frac{34}{3}\left[C_2(G_i)\right]^2\delta_{ij} + \kappa\left[4C_2(F_j) + \frac{20}{3}\delta_{ij}C_2(G_i)\right]S_2(F_i) \\ &+ \eta\left[2C_2(S_j) + \frac{1}{3}\delta_{ij}C_2(G_i)\right]S_2(S_i). \end{aligned} \tag{6.9}$$

Here, S_2 and C_2 denote the Dynkin indices and quadratic Casimir of a given representation, along with their respective multiplicity factors. For Dirac (Weyl) fermion, $\kappa = 1$ $(\kappa = \frac{1}{2})$. The parameter η takes values 1 for real scalar fields and 2 for complex scalar fields. The symbols G, F, and S represent gauge multiplets, fermions, and scalars, respectively.

At the GUT scale, the appropriate matching conditions read [121, 122]

$$\alpha^{-1}_{4C,\rm PS} = \alpha^{-1}_{2L,\rm PS} = \alpha^{-1}_{2R,\rm PS} = \alpha^{-1}_{\rm GUT}, \tag{6.10}$$

whereas, at the PS scale, we have

$$\alpha^{-1}_{3C,\rm SM} = \alpha^{-1}_{4C,\rm PS} - \frac{1}{12\pi}, \tag{6.11}$$

$$\alpha^{-1}_{2L,\rm SM} = \alpha^{-1}_{2L,\rm PS}, \tag{6.12}$$

$$\alpha^{-1}_{1Y,\rm SM} = \frac{3}{5}\left(\alpha^{-1}_{2R,\rm PS} - \frac{1}{6\pi}\right) + \frac{2}{5}\left(\alpha^{-1}_{4C,\rm PS} - \frac{1}{3\pi}\right). \tag{6.13}$$

JHEP10(2024)190

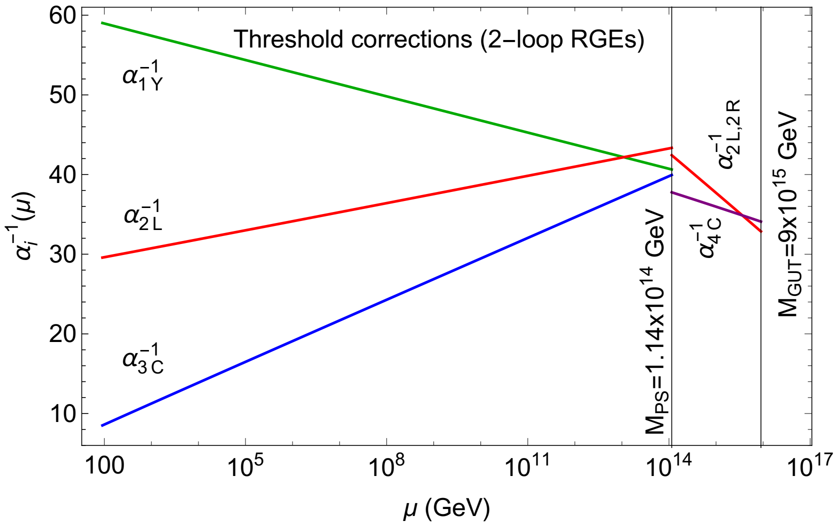

Figure 3. Example of 2-loop gauge coupling unification including 1-loop threshold corrections; see text for details.

The well-known beta function coefficients of the SM are as follows:

$$\left(b_{1Y}^{\mathrm{SM}}, b_{2L}^{\mathrm{SM}}, b_{3C}^{\mathrm{SM}}\right) = \left(\frac{41}{10}, -\frac{19}{6}, -7\right), \quad b_{ij}^{\mathrm{SM}} = \begin{pmatrix} \frac{199}{50} & \frac{27}{10} & \frac{44}{5} \\ \frac{9}{10} & \frac{35}{6} & 12 \\ \frac{11}{10} & \frac{9}{2} & -26 \end{pmatrix}. \tag{6.14}$$

If the extended survival hypothesis is assumed (as we do), the minimal set of scalar fields that affects the running above the intermediate scale is $(1,2,2)_{\mathcal{R}} \subset 10_H$, $(1,2,2)_{\mathcal{R}}$, $(15,2,2)_{\mathcal{R}} \subset 120_H$, and $(1,2,2), (15,2,2), (10,1,3), (\overline{10},3,1) \subset \overline{126}_H$. Here, for clarity, real representations are denoted by a subscript $\mathcal{R}$. The $(10,1,3) \subset \overline{126}_H$ must survive down to M_{int} as it is responsible for the PS symmetry breaking. The $(\overline{10},3,1)$ fragment should then be also at M_{int} since it is the Z_2 parity partner of $(\overline{10},3,1)$, with the discrete Z_2 parity broken only at M_{int}. The light Higgs doublet of the SM is a well-tempered mixture of the Higgs doublets from the other fragments listed above, all of which should survive down to M_{int}. With this particle content, we obtain the following beta function coefficients effective in the momentum range $M_{\mathrm{int}} \leq \mu \leq M_{\mathrm{GUT}}$:

$$\left(b_{2L}^{\mathrm{PS}}, b_{2R}^{\mathrm{PS}}, b_{4C}^{\mathrm{PS}}\right) = \left(\frac{23}{2}, \frac{23}{2}, \frac{10}{3}\right), \quad b_{ij}^{\mathrm{PS}} = \begin{pmatrix} \frac{593}{2} & \frac{147}{2} & \frac{1485}{2} \\ \frac{147}{2} & \frac{593}{2} & \frac{1485}{2} \\ \frac{297}{2} & \frac{297}{2} & \frac{4447}{6} \end{pmatrix}. \tag{6.15}$$

We have plotted in figure 2 the evolution of the gauge couplings with energy in this scenario using the full two-loop evolution equations with the assumption that all particles at the intermediate scale have a common mass, and all GUT scale particles also have a common mass. As can be seen from figure 2, the GUT scale obtained with these assumptions, $M_{\mathrm{GUT}} = 8.54 \times 10^{14}\,\mathrm{GeV}$, is not large enough to evade the current proton decay limits from Super-Kamiokande. Utilizing eq. (6.1) and using $g_{\mathrm{GUT}} = 0.586$ corresponding to figure 2, we obtain $\tau_p = 8.4 \times 10^{30}$ yrs, which is too rapid.

Our assumption in figure 2 that all GUT scale particles have a commons mass, and similarly, all intermediate scale particles are also degenerate is in fact too simplistic. The intermediate scale gauge boson spectrum discussed earlier shows clearly that the gauge bosons don't have a common mass, although their masses are close to each other. Similarly, a full Higgs potential analysis would reveal that the scalar sub-multiplets have differing masses, which holds for the particles at the GUT scale as well as at the intermediate scale. A more realistic scenario would allow for small deviations from degeneracy for these masses. These threshold corrects [121, 122] at $M_{\rm GUT}$ and $M_{\rm int}$ will play a crucial role in the gauge coupling evolution, in particular, in the numerical determination of $M_{\rm GUT}$. Therefore, in search of a viable scenario, we consider a more general scheme, where the particle content is taken to be similar to the minimal scheme, with only the scalar states $(1,2,2)_{\mathcal{R}} \subset 10_H$, $(1,2,2)_{\mathcal{R}}, (15,2,2)_{\mathcal{R}} \subset 120_H$, and $(1,2,2), (15,2,2), (10,1,3), (\overline{10},3,1) \subset \overline{126}_H$ residing close to the intermediate scale. However, these states are now allowed to live within a narrow range $(0.1-2) \times M_{\rm int}$. Similarly, states that were assumed to be perfectly degenerate with the GUT scale are now allowed to float within $(0.1-2) \times M_{\rm GUT}$. (The upper range of 2 is used to ensure that perturbation theory remains valid [112].) Due to these threshold effects, the modified matching condition between the gauge couplings α_d^{-1} of the daughter gauge group (G_d) and the gauge couplings α_p^{-1} of the parent group (G_p) reads

$$\alpha_d^{-1}(\mu) - \frac{C_2(G_d)}{12\pi} = \left(\alpha_p^{-1}(\mu) - \frac{C_2(G_p)}{12\pi}\right) - \frac{\Lambda_d(\mu)}{12\pi}, \tag{6.16}$$

where the 1-loop threshold corrections involving the superheavy fields are given by [112, 121–124],

$$\Lambda_d(\mu) = -21\ \mathrm{Tr}(t_{dV}^2 \ln\frac{m_V}{\mu}) + 2\ \eta\ \mathrm{Tr}(t_{dS}^2 \ln\frac{m_S}{\mu}) + 8\ \kappa\ \mathrm{Tr}(t_{dF}^2 \ln\frac{m_F}{\mu}). \tag{6.17}$$

Here, t_{dV}, t_{dS}, and t_{dF} are the generators for the representations of the superheavy vector, scalar, and fermion fields under G_d, respectively, with m_V, m_S, and m_F representing their corresponding masses.

For a sample particle spectrum (benchmark given below[6]), gauge coupling unification is presented in figure 3. This plot illustrates that with the inclusion of threshold corrections in the range (0.1, 2), a high GUT scale of $M_{\rm GUT} \sim 10^{16}$ GeV can be obtained, which escapes the present proton decay bounds. The corresponding intermediate scale $M_{\rm int} \sim 10^{14}$ GeV also aligns well with the fermion mass fit. Again, utilizing eq. (6.1) and using $g_{\rm GUT} = 0.615$ corresponding to figure 3, we obtain $\tau_p = 7 \times 10^{34}$ yrs, which can be probed by the 10-years of Hyper-Kamiokande [125] operations (note that the future sensitivity of Hyper-K in its 10(20)-years of operations is 7.8×10^{34} (1.56×10^{35}) yrs at 90% confidence level). The benchmark point corresponding to figure 3 has the following threshold corrections at the GUT scale:

$$\left(r_{10}^{(6,1,1)}, r_{54}^{(1,3,3)}, r_{54}^{(20',1,1)}, r_{54}^{(6,3,1),(6,1,3)}\right) = (0.11, 1.93, 0.10, 1.94), \tag{6.18}$$

$$\left(r_{120}^{(10,1,1),(\overline{10},1,1)}, r_{\overline{126}}^{(6,1,1)}\right) = (0.10, 0.11). \tag{6.19}$$

Here we have defined $r_Y^X \equiv M_Y^X/\mu$, where M_Y^X denotes the mass of the associated sub-multiplet and $\mu = M_{\rm GUT}$ for GUT-scale threshold effects and $\mu = M_{\rm int}$ for intermediate-scale

[6]The threshold corrections presented here are some examples, they are not predictions of the model. One could choose them differently, and in some cases the spectrum would be inconsistent with proton decay.

JHEP10(2024)190

threshold effects. We assume that the masses of these sub-multiplets are independent, except for the relations dictated by the Z_2-parity symmetry. This appears to be justified, since the scalar potential of the model has sufficient number of free parameters. For GUT-scale threshold effects, X in r_Y^X represents the PS sub-multiplet residing in a GUT multiplet Y. The benchmark point also takes the threshold effects at $M_{\rm int}$ to be

$$\begin{aligned}
\left(r_{120}^{(3,2,7/6)}, r_{120}^{(3,2,-1/6)}, r_{120}^{(8,2,1/2)}, r_{\overline{126}}^{(1,3,1)}\right) &= (1.73, 0.153, 0.102, 1.90),\\
\left(r_{\overline{126}}^{(\overline{3},3,1/3)}, r_{\overline{126}}^{(\overline{6},3,-1/3)}, r_{\overline{126}}^{(1,1,-2)}, r_{\overline{126}}^{(3,1,2/3)}\right) &= (1.95, 0.985, 1.82, 0.108),\\
\left(r_{\overline{126}}^{(3,1,-1/3)}, r_{\overline{126}}^{(3,1,-4/3)}, r_{\overline{126}}^{(6,1,4/3)}, r_{\overline{126}}^{(6,1,1/3)}\right) &= (0.121, 1.99, 1.40, 0.102),\\
\left(r_{\overline{126}}^{(6,1,-2/3)}, r_{\overline{126}}^{(3,2,7/6)}, r_{\overline{126}}^{(3,2,-1/6)}, r_{\overline{126}}^{(8,2,1/2)}\right) &= (0.103, 1.84, 0.112, 0.105). \qquad (6.20)
\end{aligned}$$

Here $\mu = M_{\rm int}$ and x in r_Y^X represents the SM sub-multiplet X residing in a GUT multiplet Y. The explicit form of the GUT scale threshold corrections are given as

$$\Lambda_{2L,\rm PS} = 6\ln\left(r_{54}^{(1,3,3)}\right) + 12\ln\left(r_{54}^{(6,3,1)}\right), \qquad (6.21)$$

$$\Lambda_{2R,\rm PS} = 6\ln\left(r_{54}^{(1,3,3)}\right) + 12\ln\left(r_{54}^{(6,1,3)}\right), \qquad (6.22)$$

$$\begin{aligned}
\Lambda_{4C,\rm PS} = {}& \ln\left(r_{10}^{(6,1,1)}\right) + 3\ln\left(r_{120}^{(10,1,1)}\right) + 3\ln\left(r_{120}^{(\overline{10},1,1)}\right) + 8\ln\left(r_{54}^{(20',1,1)}\right)\\
&+ 3\ln\left(r_{54}^{(6,3,1)}\right) + 3\ln\left(r_{54}^{(6,1,3)}\right) + 2\ln\left(r_{\overline{126}}^{(6,1,1)}\right). \qquad (6.23)
\end{aligned}$$

Similarly, the threshold corrections at PS scale are given by

$$\begin{aligned}
\frac{5}{3}\Lambda_{1Y,\rm SM} = {}& \frac{49}{3}\ln\left(r_{120}^{(3,2,7/6)}\right) + \frac{1}{3}\ln\left(r_{120}^{(3,2,-1/6)}\right) + 8\ln\left(r_{120}^{(8,2,1/2)}\right) + 6\ln\left(r_{\overline{126}}^{(1,3,1)}\right)\\
&+ 2\ln\left(r_{\overline{126}}^{(\overline{3},3,1/3)}\right) + 4\ln\left(r_{\overline{126}}^{(\overline{6},3,-1/3)}\right) + 8\ln\left(r_{\overline{126}}^{(1,1,-2)}\right) + \frac{8}{3}\ln\left(r_{\overline{126}}^{(3,1,2/3)}\right)\\
&+ \frac{2}{3}\ln\left(r_{\overline{126}}^{(3,1,-1/3)}\right) + \frac{32}{3}\ln\left(r_{\overline{126}}^{(3,1,-4/3)}\right) + \frac{64}{3}\ln\left(r_{\overline{126}}^{(6,1,4/3)}\right) + \frac{4}{3}\ln\left(r_{\overline{126}}^{(6,1,1/3)}\right)\\
&+ \frac{16}{3}\ln\left(r_{\overline{126}}^{(6,1,-2/3)}\right) + \frac{49}{3}\ln\left(r_{\overline{126}}^{(3,2,7/6)}\right) + \frac{1}{3}\ln\left(r_{\overline{126}}^{(3,2,-1/6)}\right) + 8\ln\left(r_{\overline{126}}^{(8,2,1/2)}\right)\\
&- 21\times 6\ln\left(\frac{g_{2R}^{\rm PS}}{g_{4C}^{\rm PS}}\right), \qquad (6.24)
\end{aligned}$$

$$\begin{aligned}
\Lambda_{2L,\rm SM} = {}& 3\ln\left(r_{120}^{(3,2,7/6)}\right) + 3\ln\left(r_{120}^{(3,2,-1/6)}\right) + 8\ln\left(r_{120}^{(8,2,1/2)}\right) + 4\ln\left(r_{\overline{126}}^{(1,3,1)}\right)\\
&+ 12\ln\left(r_{\overline{126}}^{(\overline{3},3,1/3)}\right) + 24\ln\left(r_{\overline{126}}^{(\overline{6},3,-1/3)}\right) + 3\ln\left(r_{\overline{126}}^{(3,2,7/6)}\right) + 3\ln\left(r_{\overline{126}}^{(3,2,-1/6)}\right)\\
&+ 8\ln\left(r_{\overline{126}}^{(8,2,1/2)}\right), \qquad (6.25)
\end{aligned}$$

$$\begin{aligned}
\Lambda_{3C,\rm SM} = {}& 2\ln\left(r_{120}^{(3,2,7/6)}\right) + 2\ln\left(r_{120}^{(3,2,-1/6)}\right) + 12\ln\left(r_{120}^{(8,2,1/2)}\right) + 3\ln\left(r_{\overline{126}}^{(\overline{3},3,1/3)}\right)\\
&+ 15\ln\left(r_{\overline{126}}^{(\overline{6},3,-1/3)}\right) + \ln\left(r_{\overline{126}}^{(3,1,2/3)}\right) + \ln\left(r_{\overline{126}}^{(3,1,-1/3)}\right) + \ln\left(r_{\overline{126}}^{(3,1,-4/3)}\right)\\
&+ 5\ln\left(r_{\overline{126}}^{(6,1,4/3)}\right) + 5\ln\left(r_{\overline{126}}^{(6,1,1/3)}\right) + 5\ln\left(r_{\overline{126}}^{(6,1,-2/3)}\right) + 2\ln\left(r_{\overline{126}}^{(3,2,7/6)}\right)\\
&+ 2\ln\left(r_{\overline{126}}^{(3,2,-1/6)}\right) + 12\ln\left(r_{\overline{126}}^{(8,2,1/2)}\right). \qquad (6.26)
\end{aligned}$$

Finally, summarizing the results obtained in this section, we have shown that with the assumption of extended survival hypothesis without allowing for threshold corrections, proton decay is too rapid, therefore does not lead to a viable scenario. However, there is no a priori reason for all states to be perfectly degenerate in mass with the corresponding scales, namely $M_{\rm GUT}$ and $M_{\rm int}$. Once these threshold corrections are included by assuming that the associated states can reside within a factor of $(0.1-2)$ of the corresponding scales, proton lifetime is found to be fully consistent with current limits. Interestingly, the model prefers the lifetime to be on the lower end, and the upcoming Hyper-Kamiokande experiment is expected to probe such a scenario.

7 Conclusions

In this work, we have presented a simultaneous fit to the fermion masses and mixings, including neutrino oscillation parameters, and the baryon asymmetry of the Universe generated by leptogeneis, in the context of SO(10) grand unified theory with a very minimal Yukawa sector. The model employs three scalar fields taking part in the fermion mass generation: a real 10_H, a real 120_H and a complex $\overline{126}_H$. This is the simplest Higgs system in a renormalizable SO(10) theory which does not rely of exterior symmetries such as U(1) or CP to reduce the fermion sector parameters. The framework has 15 moduli and 12 phases that enters into the fermion masses and mixings.

We have shown that excellent fits to the fermion observables can be realized with $\chi^2 = 1.45$ for the normal ordering of neutrino masses (NO) and $\chi^2 = 5.76$ for the inverted ordering (IO) case, while also generating the baryon asymmetry with the correct sign and the right value. Interestingly, the mass spectrum of the right-handed neutrinos in both NO and IO cases is found from the fermion fits to be $(M_1, M_2, M_3) \sim (10^{4-5}, 10^{11-12}, 10^{14-15})$ GeV, which leads to a scenario where $B-L$ asymmetry is dominantly produced from N_2 dynamics while N_1 is responsible for erasing the excess asymmetry. For the best-fit points, the efffective mass for neutrinoless double beta decay parameter is 3.68 (34.36) meV for NO (IO) case, consistent with the current experimental limit from KamLAND-Zen (corresponding to upper limits on $\langle m_{\beta\beta}\rangle$ of 36–156 meV [126]) while the IO scenario can be completely probed in the future nEXO experiment [127]. For the case of normal ordering of neutrino masses, the model prefers the leptonic CP-violating phase to be in the range $\delta_{\rm CP} \simeq (230-300)^\circ$. Moreover, we have found that the fermion mass fit prefers a high scale symmetry breaking triggered by a 54_H-dimensional representation. Our detailed numerical study reveals that non-zero threshold corrections are vital in realizing gauge coupling unification while being consistent with proton decay bounds. As long as these threshold correctins remain small, proton lifetime cannot exceed 10^{35} years, which may be within reach of forthcoming experiments.

Acknowledgments

The work of KSB is supported in part by the U.S. Department of Energy under grant number DE-SC0016013. CSF acknowledges the support by Fundacão de Amparo à Pesquisa do Estado de São Paulo (FAPESP) Contracts No. 2019/11197-6 and 2022/00404-3 and Conselho Nacional de Desenvolvimento Científico e Tecnológico (CNPq) under Contract No.

JHEP10(2024)190

304917/2023-0. KB, CSF and SS would also like to thanks the hospitality of Fermilab in the period from May to September, 2017 (with CSF supported by FAPESP 2017/02747-7) where this work was first initiated. They also acknowledge the Center for Theoretical Underground Physics and Related Areas (CETUP* 2024) and the Institute for Underground Science at Sanford Underground Research Facility (SURF) for providing a conducive environment for the finalization of this work. PDB wishes to thank Xubin Hu for useful discussions and acknowledges support from the Munich Institute for Astro-Particle and BioPhysics (MIAPbP) funded by the Deutsche Forschungsgemeinschaft (DFG, German Research Foundation) under Germany's Excellence Strategy – EXC-2094 – 390783311.

A Fit parameters: normal ordering

In this appendix we provide the fit parameters defined in eqs. (2.8)–(2.9) for the normal ordering (NO) solution. The best fit values of these parameters at the GUT scale are as follows:

$$r_1 = -3.23303 \times 10^{-3} + 6.51103 \times 10^{-6} i, \tag{A.1}$$

$$r_2 = -0.355963 + 1.25289 i, \tag{A.2}$$

$$\phi = -1.35108, \tag{A.3}$$

$$c_R = 9.84658 \times 10^{12}, \tag{A.4}$$

$$S = \begin{pmatrix} 6.67309 \times 10^{-9} & 0 & 0 \\ 0 & 0.211339 & 0 \\ 0 & 0 & 82.3132 \end{pmatrix} \text{GeV}, \tag{A.5}$$

$$D = \begin{pmatrix} -2.89062 \times 10^{-4} + 4.87101 \times 10^{-4} i & 2.34361 \times 10^{-3} + 3.43972 \times 10^{-3} i & -5.44162 \times 10^{-3} + 3.42227 \times 10^{-4} i \\ 2.34361 \times 10^{-3} + 3.43972 \times 10^{-3} i & 4.61704 \times 10^{-2} - 1.39879 \times 10^{-3} i & -4.37217 \times 10^{-3} - 5.40885 \times 10^{-1} i \\ -5.44162 \times 10^{-3} + 3.42227 \times 10^{-4} i & -4.37217 \times 10^{-3} - 5.40885 \times 10^{-1} i & 3.83674 \times 10^{-1} + 2.9757 \times 10^{-2} i \end{pmatrix} \text{GeV}, \tag{A.6}$$

$$A = \begin{pmatrix} 0 & 1.10335 \times 10^{-3} + 2.93066 \times 10^{-3} i & -4.7391 \times 10^{-3} - 1.62764 \times 10^{-4} i \\ -1.10335 \times 10^{-3} - 2.93066 \times 10^{-3} i & 0 & 5.35481 \times 10^{-1} - 1.00172 \times 10^{-1} i \\ 4.7391 \times 10^{-3} + 1.62764 \times 10^{-4} i & -5.35481 \times 10^{-1} + 1.00172 \times 10^{-1} i & 0 \end{pmatrix} \text{GeV}. \tag{A.7}$$

B Fit parameters: inverted ordering

In this appendix we provide the fit parameters defined in eqs. (2.8)–(2.9) for the inverted ordering (IO) solution. The best fit values of these parameters at the GUT scale are as follows:

$$r_1 = 3.72884 \times 10^{-3} + 3.49392 \times 10^{-5} i, \tag{B.1}$$

$$r_2 = 0.146324 + 1.11548 i, \tag{B.2}$$

$$\phi = -1.55817, \tag{B.3}$$

$$c_R = 7.01764 \times 10^{12}, \tag{B.4}$$

$$S = \begin{pmatrix} 1.51614 \times 10^{-9} & 0 & 0 \\ 0 & 2.45908 \times 10^{-1} & 0 \\ 0 & 0 & 8.34044 \times 10^{1} \end{pmatrix} \text{ GeV}, \tag{B.5}$$

$$D = \begin{pmatrix} -7.18337 \times 10^{-4} + 2.32015 \times 10^{-4} i & 2.67684 \times 10^{-3} + 1.98135 \times 10^{-3} i & -3.98144 \times 10^{-3} + 8.5517 \times 10^{-4} i \\ 2.67684 \times 10^{-3} + 1.98135 \times 10^{-3} i & 6.6873 \times 10^{-3} - 4.28609 \times 10^{-2} i & -4.34152 \times 10^{-2} - 5.38267 \times 10^{-1} i \\ -3.98144 \times 10^{-3} + 8.5517 \times 10^{-4} i & -4.34152 \times 10^{-2} - 5.38267 \times 10^{-1} i & -3.33469 \times 10^{-1} - 3.11386 \times 10^{-2} i \end{pmatrix} \text{ GeV}, \tag{B.6}$$

$$A = \begin{pmatrix} 0 & 2.69205 \times 10^{-3} + 1.37192 \times 10^{-3} i & -3.46624 \times 10^{-3} + 7.82184 \times 10^{-4} i \\ -2.69205 \times 10^{-3} - 1.37192 \times 10^{-3} i & 0 & 5.54677 \times 10^{-1} - 3.55935 \times 10^{-2} i \\ 3.46624 \times 10^{-3} - 7.82184 \times 10^{-4} i & -5.54677 \times 10^{-1} + 3.55935 \times 10^{-2} i & 0 \end{pmatrix} \text{ GeV}. \tag{B.7}$$

C Parameters for leptogenesis

For the convenience of the reader, here we present the neutrino Dirac, eq. (2.12), and the charged lepton, eq. (2.11), Yukawa coupling matrices in a basis where the right-handed neutrino mass matrix, eq. (2.13), is diagonal. These quantities are given at the M_2 scale used for leptogenesis and at M_1 scale used for washout calculations. Notice that in our flavor-covariant formalism, it is not necessary to use the charged lepton mass diagonal basis. As we have shown in section 3, B or $B-L$ asymmetry is invariant under flavor rotations, see eq. (3.19). These Yukawa coupling and masses quoted below are the outcomes of the fits presented in appendices A and B. At renormalization scale M_2, we have for

normal ordering (NO):

$$(M_1, M_2, M_3) = \left(6.57071 \times 10^{4}, 2.08095 \times 10^{12}, 7.51307 \times 10^{14}\right) \text{ GeV}, \tag{C.1}$$

$$y_{\nu_D} = \begin{pmatrix} -1.60399 \times 10^{-6} + 2.70269 \times 10^{-6} i & 3.83439 \times 10^{-6} - 1.6047 \times 10^{-6} i & 3.99098 \times 10^{-6} + 1.09775 \times 10^{-6} i \\ 2.21767 \times 10^{-5} + 3.97769 \times 10^{-5} i & -3.26201 \times 10^{-3} - 7.64731 \times 10^{-6} i & -3.77518 \times 10^{-3} - 2.01867 \times 10^{-3} i \\ -6.07975 \times 10^{-5} + 2.51138 \times 10^{-6} i & 3.58336 \times 10^{-3} - 3.71946 \times 10^{-3} i & -1.29043 + 1.55752 \times 10^{-4} i \end{pmatrix}, \tag{C.2}$$

$$y_E = \begin{pmatrix} -1.6569 \times 10^{-6} + 2.79187 \times 10^{-6} i & -9.85534 \times 10^{-6} + 2.16613 \times 10^{-5} i & -2.15379 \times 10^{-5} - 3.35986 \times 10^{-5} i \\ 3.67292 \times 10^{-5} + 1.77743 \times 10^{-5} i & 2.76287 \times 10^{-4} - 8.26329 \times 10^{-6} i & -4.2159 \times 10^{-4} + 1.00513 \times 10^{-3} i \\ -4.20094 \times 10^{-5} + 3.56618 \times 10^{-5} i & 3.46994 \times 10^{-4} - 7.14891 \times 10^{-3} i & 7.17039 \times 10^{-3} + 1.71882 \times 10^{-4} i \end{pmatrix}. \tag{C.3}$$

and for inverted ordering (IO):

$$(M_1, M_2, M_3) = \left(1.06397 \times 10^{4}, 1.72569 \times 10^{12}, 5.37463 \times 10^{14}\right) \text{ GeV}, \tag{C.4}$$

$$y_{\nu_D} = \begin{pmatrix} -3.96655 \times 10^{-6} + 1.28114 \times 10^{-6} i & -5.56661 \times 10^{-7} + 1.20903 \times 10^{-7} i & 2.06712 \times 10^{-8} + 2.91964 \times 10^{-6} i \\ 3.01215 \times 10^{-5} + 2.17624 \times 10^{-5} i & -4.03696 \times 10^{-3} - 2.36699 \times 10^{-4} i & -3.60534 \times 10^{-3} - 3.17552 \times 10^{-3} i \\ -4.12295 \times 10^{-5} + 6.06392 \times 10^{-6} i & 3.00083 \times 10^{-3} - 2.53226 \times 10^{-3} i & -1.29604 - 1.61077 \times 10^{-4} i \end{pmatrix}, \tag{C.5}$$

$$y_E = \begin{pmatrix} -4.10011 \times 10^{-6} + 1.32424 \times 10^{-6} i & 8.79887 \times 10^{-6} + 2.95932 \times 10^{-5} i & -3.26182 \times 10^{-5} - 1.76321 \times 10^{-5} i \\ 2.1766 \times 10^{-5} - 6.97592 \times 10^{-6} i & 2.23477 \times 10^{-5} - 2.44794 \times 10^{-4} i & 4.71227 \times 10^{-4} + 4.57941 \times 10^{-4} i \\ -1.4865 \times 10^{-5} + 2.62983 \times 10^{-5} i & -9.36539 \times 10^{-4} - 6.5749 \times 10^{-3} i & -7.70666 \times 10^{-3} - 2.41542 \times 10^{-4} i \end{pmatrix}. \tag{C.6}$$

JHEP10(2024)190

At the scale M_1, we have M_i as in eq. (C.1) and

NO :

$$y_{\nu_D} = \begin{pmatrix} -1.55316 \times 10^{-6} + 2.61706 \times 10^{-6} i & 3.71295 \times 10^{-6} - 1.55390 \times 10^{-6} i & 3.86458 \times 10^{-6} + 1.06301 \times 10^{-6} i \\ 0.0000221767 + 0.0000397769 i & -0.00326201 - 7.64730 \times 10^{-6} i & -0.00377518 - 0.00201867 i \\ -0.0000607975 + 2.51138 \times 10^{-6} i & 0.00358336 - 0.00371946 i & -1.29043 + 0.000155752 i \end{pmatrix}, \tag{C.7}$$

$$y_E = \begin{pmatrix} -1.68764 \times 10^{-6} + 2.84365 \times 10^{-6} i & -0.0000100378 + 0.0000220627 i & -0.000021937 - 0.0000342215 i \\ 0.0000374106 + 0.0000181041 i & 0.0002814 - 8.42045 \times 10^{-6} i & -0.000429407 + 0.00102376 i \\ -0.0000427879 + 0.0000363228 i & 0.000353425 - 0.00728139 i & 0.00730327 + 0.000175067 i \end{pmatrix}. \tag{C.8}$$

IO :

$$y_{\nu_D} = \begin{pmatrix} -3.80357 \times 10^{-6} + 1.2285 \times 10^{-6} i & -5.33817 \times 10^{-7} + 1.15942 \times 10^{-7} i & 1.98218 \times 10^{-8} + 2.79971 \times 10^{-6} i \\ 3.01215 \times 10^{-5} + 2.17624 \times 10^{-5} i & -4.03696 \times 10^{-3} - 2.36699 \times 10^{-4} i & -3.60534 \times 10^{-3} - 3.17552 \times 10^{-3} i \\ -4.12295 \times 10^{-5} + 6.06392 \times 10^{-6} i & 3.00083 \times 10^{-3} - 2.53226 \times 10^{-3} i & -1.29604 - 1.61077 \times 10^{-4} i \end{pmatrix}, \tag{C.9}$$

$$y_E = \begin{pmatrix} -4.15257 \times 10^{-6} + 1.34119 \times 10^{-6} i & 8.91127 \times 10^{-6} + 2.99719 \times 10^{-5} i & -3.30355 \times 10^{-5} - 1.78575 \times 10^{-5} i \\ 2.20445 \times 10^{-5} - 7.06517 \times 10^{-6} i & 2.26371 \times 10^{-5} - 2.4793 \times 10^{-4} i & 4.77254 \times 10^{-4} + 4.63796 \times 10^{-4} i \\ -1.50549 \times 10^{-5} + 2.66343 \times 10^{-5} i & -9.48504 \times 10^{-4} - 6.6589 \times 10^{-3} i & -7.80512 \times 10^{-3} - 2.44628 \times 10^{-4} i \end{pmatrix}. \tag{C.10}$$

References

[1] J.C. Pati and A. Salam, *Lepton Number as the Fourth Color*, *Phys. Rev. D* **10** (1974) 275 [INSPIRE].

[2] H. Georgi and S.L. Glashow, *Unity of All Elementary Particle Forces*, *Phys. Rev. Lett.* **32** (1974) 438 [INSPIRE].

[3] H. Georgi, H.R. Quinn and S. Weinberg, *Hierarchy of Interactions in Unified Gauge Theories*, *Phys. Rev. Lett.* **33** (1974) 451 [INSPIRE].

[4] H. Georgi, *The State of the Art — Gauge Theories*, *AIP Conf. Proc.* **23** (1975) 575 [INSPIRE].

[5] H. Fritzsch and P. Minkowski, *Unified Interactions of Leptons and Hadrons*, *Annals Phys.* **93** (1975) 193 [INSPIRE].

[6] J.C. Pati and A. Salam, *Is Baryon Number Conserved?*, *Phys. Rev. Lett.* **31** (1973) 661 [INSPIRE].

[7] P. Minkowski, *$\mu \to e\gamma$ at a Rate of One Out of 10^9 Muon Decays?*, *Phys. Lett. B* **67** (1977) 421 [INSPIRE].

[8] T. Yanagida, *Horizontal gauge symmetry and masses of neutrinos*, *Conf. Proc. C* **7902131** (1979) 95 [INSPIRE].

[9] S.L. Glashow, *The Future of Elementary Particle Physics*, *NATO Sci. Ser. B* **61** (1980) 687 [INSPIRE].

[10] M. Gell-Mann, P. Ramond and R. Slansky, *Complex Spinors and Unified Theories*, *Conf. Proc. C* **790927** (1979) 315 [arXiv:1306.4669] [INSPIRE].

[11] R.N. Mohapatra and G. Senjanovic, *Neutrino Mass and Spontaneous Parity Nonconservation*, *Phys. Rev. Lett.* **44** (1980) 912 [INSPIRE].

[12] J. Schechter and J.W.F. Valle, *Neutrino Masses in $SU(2) \times U(1)$ Theories*, *Phys. Rev. D* **22** (1980) 2227 [INSPIRE].

[13] J. Schechter and J.W.F. Valle, *Neutrino Decay and Spontaneous Violation of Lepton Number*, *Phys. Rev. D* **25** (1982) 774 [INSPIRE].

[14] M. Fukugita and T. Yanagida, *Baryogenesis Without Grand Unification*, *Phys. Lett. B* **174** (1986) 45 [INSPIRE].

[15] F.R. Klinkhamer and N.S. Manton, *A Saddle Point Solution in the Weinberg-Salam Theory*, *Phys. Rev. D* **30** (1984) 2212 [INSPIRE].

[16] P.B. Arnold and L.D. McLerran, *Sphalerons, Small Fluctuations and Baryon Number Violation in Electroweak Theory*, *Phys. Rev. D* **36** (1987) 581 [INSPIRE].

[17] P.B. Arnold and L.D. McLerran, *The Sphaleron Strikes Back*, *Phys. Rev. D* **37** (1988) 1020 [INSPIRE].

[18] W. Buchmuller, P. Di Bari and M. Plumacher, *Leptogenesis for pedestrians*, *Annals Phys.* **315** (2005) 305 [hep-ph/0401240] [INSPIRE].

[19] Y. Nir, *Introduction to leptogenesis*, in the proceedings of the *6th Rencontres du Vietnam: Challenges in Particle Astrophysics*, Hanoi, Vietnam, August 06–12 (2006) [hep-ph/0702199] [INSPIRE].

[20] S. Davidson, E. Nardi and Y. Nir, *Leptogenesis*, *Phys. Rept.* **466** (2008) 105 [arXiv:0802.2962] [INSPIRE].

[21] A. Pilaftsis, *The Little Review on Leptogenesis*, *J. Phys. Conf. Ser.* **171** (2009) 012017 [arXiv:0904.1182] [INSPIRE].

[22] P. Di Bari, *An introduction to leptogenesis and neutrino properties*, *Contemp. Phys.* **53** (2012) 315 [arXiv:1206.3168] [INSPIRE].

[23] C.S. Fong, E. Nardi and A. Riotto, *Leptogenesis in the Universe*, *Adv. High Energy Phys.* **2012** (2012) 158303 [arXiv:1301.3062] [INSPIRE].

[24] E.J. Chun et al., *Probing Leptogenesis*, *Int. J. Mod. Phys. A* **33** (2018) 1842005 [arXiv:1711.02865] [INSPIRE].

[25] P.S.B. Dev et al., *Flavor effects in leptogenesis*, *Int. J. Mod. Phys. A* **33** (2018) 1842001 [arXiv:1711.02861] [INSPIRE].

[26] D. Bodeker and W. Buchmuller, *Baryogenesis from the weak scale to the grand unification scale*, *Rev. Mod. Phys.* **93** (2021) 035004 [arXiv:2009.07294] [INSPIRE].

[27] K.S. Babu and R.N. Mohapatra, *Predictive neutrino spectrum in minimal $SO(10)$ grand unification*, *Phys. Rev. Lett.* **70** (1993) 2845 [hep-ph/9209215] [INSPIRE].

[28] B. Bajc, G. Senjanovic and F. Vissani, *How neutrino and charged fermion masses are connected within minimal supersymmetric $SO(10)$*, *PoS* **HEP2001** (2001) 198 [hep-ph/0110310] [INSPIRE].

[29] B. Bajc, G. Senjanovic and F. Vissani, *b-τ unification and large atmospheric mixing: A case for noncanonical seesaw*, *Phys. Rev. Lett.* **90** (2003) 051802 [hep-ph/0210207] [INSPIRE].

[30] T. Fukuyama and N. Okada, *Neutrino oscillation data versus minimal supersymmetric SO(10) model*, JHEP **11** (2002) 011 [hep-ph/0205066] [INSPIRE].

[31] H.S. Goh, R.N. Mohapatra and S.-P. Ng, *Minimal SUSY SO(10), b-τ unification and large neutrino mixings*, Phys. Lett. B **570** (2003) 215 [hep-ph/0303055] [INSPIRE].

[32] H.S. Goh, R.N. Mohapatra and S.-P. Ng, *Minimal SUSY SO(10) model and predictions for neutrino mixings and leptonic CP violation*, Phys. Rev. D **68** (2003) 115008 [hep-ph/0308197] [INSPIRE].

[33] S. Bertolini, M. Frigerio and M. Malinsky, *Fermion masses in SUSY SO(10) with type II seesaw: A Non-minimal predictive scenario*, Phys. Rev. D **70** (2004) 095002 [hep-ph/0406117] [INSPIRE].

[34] S. Bertolini and M. Malinsky, *On CP violation in minimal renormalizable SUSY SO(10) and beyond*, Phys. Rev. D **72** (2005) 055021 [hep-ph/0504241] [INSPIRE].

[35] K.S. Babu and C. Macesanu, *Neutrino masses and mixings in a minimal SO(10) model*, Phys. Rev. D **72** (2005) 115003 [hep-ph/0505200] [INSPIRE].

[36] S. Bertolini, T. Schwetz and M. Malinsky, *Fermion masses and mixings in SO(10) models and the neutrino challenge to SUSY GUTs*, Phys. Rev. D **73** (2006) 115012 [hep-ph/0605006] [INSPIRE].

[37] B. Bajc, I. Dorsner and M. Nemevsek, *Minimal SO(10) splits supersymmetry*, JHEP **11** (2008) 007 [arXiv:0809.1069] [INSPIRE].

[38] A.S. Joshipura and K.M. Patel, *Fermion Masses in SO(10) Models*, Phys. Rev. D **83** (2011) 095002 [arXiv:1102.5148] [INSPIRE].

[39] G. Altarelli and D. Meloni, *A non supersymmetric SO(10) grand unified model for all the physics below M_{GUT}*, JHEP **08** (2013) 021 [arXiv:1305.1001] [INSPIRE].

[40] A. Dueck and W. Rodejohann, *Fits to SO(10) Grand Unified Models*, JHEP **09** (2013) 024 [arXiv:1306.4468] [INSPIRE].

[41] T. Fukuyama, K. Ichikawa and Y. Mimura, *Revisiting fermion mass and mixing fits in the minimal SUSY SO(10) GUT*, Phys. Rev. D **94** (2016) 075018 [arXiv:1508.07078] [INSPIRE].

[42] K.S. Babu, B. Bajc and S. Saad, *New Class of SO(10) Models for Flavor*, Phys. Rev. D **94** (2016) 015030 [arXiv:1605.05116] [INSPIRE].

[43] K.S. Babu, B. Bajc and S. Saad, *Yukawa Sector of Minimal SO(10) Unification*, JHEP **02** (2017) 136 [arXiv:1612.04329] [INSPIRE].

[44] K.S. Babu, B. Bajc and S. Saad, *Resurrecting Minimal Yukawa Sector of SUSY SO(10)*, JHEP **10** (2018) 135 [arXiv:1805.10631] [INSPIRE].

[45] K.S. Babu, T. Fukuyama, S. Khan and S. Saad, *Peccei-Quinn Symmetry and Nucleon Decay in Renormalizable SUSY SO(10)*, JHEP **06** (2019) 045 [arXiv:1812.11695] [INSPIRE].

[46] T. Ohlsson and M. Pernow, *Running of Fermion Observables in Non-Supersymmetric SO(10) Models*, JHEP **11** (2018) 028 [arXiv:1804.04560] [INSPIRE].

[47] T. Ohlsson and M. Pernow, *Fits to Non-Supersymmetric SO(10) Models with Type I and II Seesaw Mechanisms Using Renormalization Group Evolution*, JHEP **06** (2019) 085 [arXiv:1903.08241] [INSPIRE].

[48] K.S. Babu and S. Saad, *Flavor Hierarchies from Clockwork in SO(10) GUT*, Phys. Rev. D **103** (2021) 015009 [arXiv:2007.16085] [INSPIRE].

JHEP10(2024)190

[49] V.S. Mummidi and K.M. Patel, *Leptogenesis and fermion mass fit in a renormalizable $SO(10)$ model*, *JHEP* **12** (2021) 042 [arXiv:2109.04050] [INSPIRE].

[50] S. Saad, *Probing minimal grand unification through gravitational waves, proton decay, and fermion masses*, *JHEP* **04** (2023) 058 [arXiv:2212.05291] [INSPIRE].

[51] N. Haba, Y. Shimizu and T. Yamada, *Neutrino Mass in Non-Supersymmetric $SO(10)$ GUT*, *Phys. Rev. D* **108** (2023) 095005 [arXiv:2304.06263] [INSPIRE].

[52] A. Kaladharan and S. Saad, *Fermion mass, axion dark matter, and leptogenesis in $SO(10)$ GUT*, *Phys. Rev. D* **109** (2024) 055010 [arXiv:2308.04497] [INSPIRE].

[53] F. Vissani, *Do experiments suggest a hierarchy problem?*, *Phys. Rev. D* **57** (1998) 7027 [hep-ph/9709409] [INSPIRE].

[54] J.A. Casas, J.R. Espinosa and I. Hidalgo, *Implications for new physics from fine-tuning arguments. I. Application to SUSY and seesaw cases*, *JHEP* **11** (2004) 057 [hep-ph/0410298] [INSPIRE].

[55] W. Buchmuller and M. Plumacher, *Baryon asymmetry and neutrino mixing*, *Phys. Lett. B* **389** (1996) 73 [hep-ph/9608308] [INSPIRE].

[56] E. Nezri and J. Orloff, *Neutrino oscillations versus leptogenesis in $SO(10)$ models*, *JHEP* **04** (2003) 020 [hep-ph/0004227] [INSPIRE].

[57] F. Buccella, D. Falcone and F. Tramontano, *Baryogenesis via leptogenesis in $SO(10)$ models*, *Phys. Lett. B* **524** (2002) 241 [hep-ph/0108172] [INSPIRE].

[58] G.C. Branco, R. Gonzalez Felipe, F.R. Joaquim and M.N. Rebelo, *Leptogenesis, CP violation and neutrino data: What can we learn?*, *Nucl. Phys. B* **640** (2002) 202 [hep-ph/0202030] [INSPIRE].

[59] E.K. Akhmedov, M. Frigerio and A.Y. Smirnov, *Probing the seesaw mechanism with neutrino data and leptogenesis*, *JHEP* **09** (2003) 021 [hep-ph/0305322] [INSPIRE].

[60] P. Di Bari and A. Riotto, *Successful type I Leptogenesis with $SO(10)$-inspired mass relations*, *Phys. Lett. B* **671** (2009) 462 [arXiv:0809.2285] [INSPIRE].

[61] P. Di Bari and A. Riotto, *Testing $SO(10)$-inspired leptogenesis with low energy neutrino experiments*, *JCAP* **04** (2011) 037 [arXiv:1012.2343] [INSPIRE].

[62] F. Buccella et al., *Squeezing out predictions with leptogenesis from $SO(10)$*, *Phys. Rev. D* **86** (2012) 035012 [arXiv:1203.0829] [INSPIRE].

[63] P. Di Bari and L. Marzola, *$SO(10)$-inspired solution to the problem of the initial conditions in leptogenesis*, *Nucl. Phys. B* **877** (2013) 719 [arXiv:1308.1107] [INSPIRE].

[64] P. Di Bari, L. Marzola and M. Re Fiorentin, *Decrypting $SO(10)$-inspired leptogenesis*, *Nucl. Phys. B* **893** (2015) 122 [arXiv:1411.5478] [INSPIRE].

[65] P. Di Bari and S.F. King, *Successful N_2 leptogenesis with flavour coupling effects in realistic unified models*, *JCAP* **10** (2015) 008 [arXiv:1507.06431] [INSPIRE].

[66] P. Di Bari and M. Re Fiorentin, *A full analytic solution of $SO(10)$-inspired leptogenesis*, *JHEP* **10** (2017) 029 [arXiv:1705.01935] [INSPIRE].

[67] M. Chianese and P. Di Bari, *Strong thermal $SO(10)$-inspired leptogenesis in the light of recent results from long-baseline neutrino experiments*, *JHEP* **05** (2018) 073 [arXiv:1802.07690] [INSPIRE].

[68] P. Di Bari and R. Samanta, *The $SO(10)$-inspired leptogenesis timely opportunity*, *JHEP* **08** (2020) 124 [arXiv:2005.03057] [INSPIRE].

[69] P. Di Bari, *Seesaw geometry and leptogenesis*, *Nucl. Phys. B* **727** (2005) 318 [hep-ph/0502082] [INSPIRE].

[70] O. Vives, *Flavor dependence of CP asymmetries and thermal leptogenesis with strong right-handed neutrino mass hierarchy*, *Phys. Rev. D* **73** (2006) 073006 [hep-ph/0512160] [INSPIRE].

[71] C.S. Fong, D. Meloni, A. Meroni and E. Nardi, *Leptogenesis in $SO(10)$*, *JHEP* **01** (2015) 111 [arXiv:1412.4776] [INSPIRE].

[72] K.M. Patel, *Minimal spontaneous CP-violating GUT and predictions for leptonic CP phases*, *Phys. Rev. D* **107** (2023) 075041 [arXiv:2212.04095] [INSPIRE].

[73] *Nufit webpage*, October (2021) [http://www.nu-fit.org/?q=node/238].

[74] C.S. Fong, *Cosmic evolution of lepton flavor charges*, *Phys. Rev. D* **105** (2022) 043004 [arXiv:2109.04478] [INSPIRE].

[75] W. Buchmuller and M. Plumacher, *Spectator processes and baryogenesis*, *Phys. Lett. B* **511** (2001) 74 [hep-ph/0104189] [INSPIRE].

[76] E. Nardi, Y. Nir, J. Racker and E. Roulet, *On Higgs and sphaleron effects during the leptogenesis era*, *JHEP* **01** (2006) 068 [hep-ph/0512052] [INSPIRE].

[77] B. Garbrecht, F. Glowna and P. Schwaller, *Scattering Rates For Leptogenesis: Damping of Lepton Flavour Coherence and Production of Singlet Neutrinos*, *Nucl. Phys. B* **877** (2013) 1 [arXiv:1303.5498] [INSPIRE].

[78] B. Garbrecht and P. Schwaller, *Spectator Effects during Leptogenesis in the Strong Washout Regime*, *JCAP* **10** (2014) 012 [arXiv:1404.2915] [INSPIRE].

[79] M. D'Onofrio, K. Rummukainen and A. Tranberg, *Sphaleron Rate in the Minimal Standard Model*, *Phys. Rev. Lett.* **113** (2014) 141602 [arXiv:1404.3565] [INSPIRE].

[80] C.S. Fong, *Baryogenesis from Symmetry Principle*, *Phys. Lett. B* **752** (2016) 247 [arXiv:1508.03648] [INSPIRE].

[81] S. Blanchet, P. Di Bari, D.A. Jones and L. Marzola, *Leptogenesis with heavy neutrino flavours: from density matrix to Boltzmann equations*, *JCAP* **01** (2013) 041 [arXiv:1112.4528] [INSPIRE].

[82] C.S. Fong, *Baryogenesis in the Standard Model and its Supersymmetric Extension*, *Phys. Rev. D* **103** (2021) L051705 [arXiv:2012.03973] [INSPIRE].

[83] A. Salvio, P. Lodone and A. Strumia, *Towards leptogenesis at NLO: the right-handed neutrino interaction rate*, *JHEP* **08** (2011) 116 [arXiv:1106.2814] [INSPIRE].

[84] M. Laine and Y. Schroder, *Thermal right-handed neutrino production rate in the non-relativistic regime*, *JHEP* **02** (2012) 068 [arXiv:1112.1205] [INSPIRE].

[85] B. Garbrecht, P. Klose and C. Tamarit, *Relativistic and spectator effects in leptogenesis with heavy sterile neutrinos*, *JHEP* **02** (2020) 117 [arXiv:1904.09956] [INSPIRE].

[86] S. Antusch et al., *Running neutrino mass parameters in see-saw scenarios*, *JHEP* **03** (2005) 024 [hep-ph/0501272] [INSPIRE].

[87] Super-Kamiokande collaboration, *Search for proton decay via $p \to e^+\pi^0$ and $p \to \mu^+\pi^0$ with an enlarged fiducial volume in Super-Kamiokande I-IV*, Phys. Rev. D **102** (2020) 112011 [arXiv:2010.16098] [inSPIRE].

[88] Planck collaboration, *Planck 2018 results. VI. Cosmological parameters*, Astron. Astrophys. **641** (2020) A6 [*Erratum ibid.* **652** (2021) C4] [arXiv:1807.06209] [inSPIRE].

[89] S. Antusch and V. Maurer, *Running quark and lepton parameters at various scales*, JHEP **11** (2013) 115 [arXiv:1306.6879] [inSPIRE].

[90] I. Esteban et al., *The fate of hints: updated global analysis of three-flavor neutrino oscillations*, JHEP **09** (2020) 178 [arXiv:2007.14792] [inSPIRE].

[91] Z.-Z. Xing, *Low-energy limits on heavy Majorana neutrino masses from the neutrinoless double-beta decay and non-unitary neutrino mixing*, Phys. Lett. B **679** (2009) 255 [arXiv:0907.3014] [inSPIRE].

[92] W. Rodejohann, *Inverse Neutrino-less Double Beta Decay Revisited: Neutrinos, Higgs Triplets and a Muon Collider*, Phys. Rev. D **81** (2010) 114001 [arXiv:1005.2854] [inSPIRE].

[93] S. Davidson and A. Ibarra, *A lower bound on the right-handed neutrino mass from leptogenesis*, Phys. Lett. B **535** (2002) 25 [hep-ph/0202239] [inSPIRE].

[94] S. Antusch, K. Hinze, S. Saad and J. Steiner, *Singling out SO(10) GUT models using recent PTA results*, Phys. Rev. D **108** (2023) 095053 [arXiv:2307.04595] [inSPIRE].

[95] H. Xu et al., *Searching for the Nano-Hertz Stochastic Gravitational Wave Background with the Chinese Pulsar Timing Array Data Release I*, Res. Astron. Astrophys. **23** (2023) 075024 [arXiv:2306.16216] [inSPIRE].

[96] EPTA and InPTA: collaborations, *The second data release from the European Pulsar Timing Array — III. Search for gravitational wave signals*, Astron. Astrophys. **678** (2023) A50 [arXiv:2306.16214] [inSPIRE].

[97] NANOGrav collaboration, *The NANOGrav 15 yr Data Set: Evidence for a Gravitational-wave Background*, Astrophys. J. Lett. **951** (2023) L8 [arXiv:2306.16213] [inSPIRE].

[98] D.J. Reardon et al., *Search for an Isotropic Gravitational-wave Background with the Parkes Pulsar Timing Array*, Astrophys. J. Lett. **951** (2023) L6 [arXiv:2306.16215] [inSPIRE].

[99] NANOGrav collaboration, *The NANOGrav 15 yr Data Set: Search for Signals from New Physics*, Astrophys. J. Lett. **951** (2023) L11 [*Erratum ibid.* **971** (2024) L27] [arXiv:2306.16219] [inSPIRE].

[100] Super-Kamiokande collaboration, *Latest results from Super-Kamiokande*, in the proceedings of the *58th Rencontres de Moriond on Electroweak Interactions and Unified Theories*, La Thuile, Italy, March 24–31 (2024) [arXiv:2405.07900] [inSPIRE].

[101] DESI collaboration, *DESI 2024 VI: Cosmological Constraints from the Measurements of Baryon Acoustic Oscillations*, arXiv:2404.03002 [inSPIRE].

[102] P.S.B. Dev et al., *Searches for baryon number violation in neutrino experiments: a white paper*, J. Phys. G **51** (2024) 033001 [arXiv:2203.08771] [inSPIRE].

[103] P. Fileviez Perez, *Fermion mixings versus $d = 6$ proton decay*, Phys. Lett. B **595** (2004) 476 [hep-ph/0403286] [inSPIRE].

[104] P. Nath and P. Fileviez Perez, *Proton stability in grand unified theories, in strings and in branes*, Phys. Rept. **441** (2007) 191 [hep-ph/0601023] [inSPIRE].

[105] Y. Aoki, T. Izubuchi, E. Shintani and A. Soni, *Improved lattice computation of proton decay matrix elements*, *Phys. Rev. D* **96** (2017) 014506 [arXiv:1705.01338] [INSPIRE].

[106] T. Nihei and J. Arafune, *The two loop long range effect on the proton decay effective Lagrangian*, *Prog. Theor. Phys.* **93** (1995) 665 [hep-ph/9412325] [INSPIRE].

[107] A.J. Buras, J.R. Ellis, M.K. Gaillard and D.V. Nanopoulos, *Aspects of the Grand Unification of Strong, Weak and Electromagnetic Interactions*, *Nucl. Phys. B* **135** (1978) 66 [INSPIRE].

[108] J.T. Goldman and D.A. Ross, *How Accurately Can We Estimate the Proton Lifetime in an $SU(5)$ Grand Unified Model?*, *Nucl. Phys. B* **171** (1980) 273 [INSPIRE].

[109] W.E. Caswell, J. Milutinovic and G. Senjanovic, *Predictions of Left-right Symmetric Grand Unified Theories*, *Phys. Rev. D* **26** (1982) 161 [INSPIRE].

[110] L.E. Ibanez and C. Munoz, *Enhancement Factors for Supersymmetric Proton Decay in the Wess-Zumino Gauge*, *Nucl. Phys. B* **245** (1984) 425 [INSPIRE].

[111] L.F. Abbott and M.B. Wise, *The Effective Hamiltonian for Nucleon Decay*, *Phys. Rev. D* **22** (1980) 2208 [INSPIRE].

[112] K.S. Babu and S. Khan, *Minimal nonsupersymmetric $SO(10)$ model: Gauge coupling unification, proton decay, and fermion masses*, *Phys. Rev. D* **92** (2015) 075018 [arXiv:1507.06712] [INSPIRE].

[113] J. Chakrabortty, R. Maji and S.F. King, *Unification, Proton Decay and Topological Defects in non-SUSY GUTs with Thresholds*, *Phys. Rev. D* **99** (2019) 095008 [arXiv:1901.05867] [INSPIRE].

[114] K.S. Babu, B. Bajc and V. Susič, *A realistic theory of E_6 unification through novel intermediate symmetries*, *JHEP* **06** (2024) 018 [arXiv:2403.20278] [INSPIRE].

[115] H. Georgi, *Towards a Grand Unified Theory of Flavor*, *Nucl. Phys. B* **156** (1979) 126 [INSPIRE].

[116] F. del Aguila and L.E. Ibanez, *Higgs Bosons in $SO(10)$ and Partial Unification*, *Nucl. Phys. B* **177** (1981) 60 [INSPIRE].

[117] R.N. Mohapatra and G. Senjanovic, *Higgs Boson Effects in Grand Unified Theories*, *Phys. Rev. D* **27** (1983) 1601 [INSPIRE].

[118] S. Dimopoulos and H.M. Georgi, *Extended Survival Hypothesis and Fermion Masses*, *Phys. Lett. B* **140** (1984) 67 [INSPIRE].

[119] S. Saad, *Fermion Masses and Mixings, Leptogenesis and Baryon Number Violation in Pati-Salam Model*, *Nucl. Phys. B* **943** (2019) 114630 [arXiv:1712.04880] [INSPIRE].

[120] M.E. Machacek and M.T. Vaughn, *Two Loop Renormalization Group Equations in a General Quantum Field Theory. I. Wave Function Renormalization*, *Nucl. Phys. B* **222** (1983) 83 [INSPIRE].

[121] S. Weinberg, *Effective Gauge Theories*, *Phys. Lett. B* **91** (1980) 51 [INSPIRE].

[122] L.J. Hall, *Grand Unification of Effective Gauge Theories*, *Nucl. Phys. B* **178** (1981) 75 [INSPIRE].

[123] S. Bertolini, L. Di Luzio and M. Malinsky, *Intermediate mass scales in the non-supersymmetric $SO(10)$ grand unification: A Reappraisal*, *Phys. Rev. D* **80** (2009) 015013 [arXiv:0903.4049] [INSPIRE].

[124] S. Bertolini, L. Di Luzio and M. Malinsky, *Light color octet scalars in the minimal $SO(10)$ grand unification*, *Phys. Rev. D* **87** (2013) 085020 [arXiv:1302.3401] [INSPIRE].

JHEP10(2024)190

[125] Hyper-Kamiokande collaboration, *Hyper-Kamiokande Design Report*, arXiv:1805.04163 [inSPIRE].

[126] KamLAND-Zen collaboration, *Search for the Majorana Nature of Neutrinos in the Inverted Mass Ordering Region with KamLAND-Zen*, *Phys. Rev. Lett.* **130** (2023) 051801 [arXiv:2203.02139] [inSPIRE].

[127] nEXO collaboration, *nEXO: neutrinoless double β decay search beyond* 10^{28} *year half-life sensitivity*, *J. Phys. G* **49** (2022) 015104 [arXiv:2106.16243] [inSPIRE].

JHEP10(2024)190